Development of a Quaternion-Based Algorithm to Process Data in Robotics Applications

Industrial Representative: J. Ashmore (TIAX)

Faculty: J.R. Buchanan (Millersville), A. Downey (Olin), D.A. Edwards (Delaware), J.D. Fehribach (WPI), J. Ockendon (Oxford, UK), C. Raymond (NJIT)

Students: K. Bhalerao (RPI), J. Cass (Olin), E. Fertig (Maryland, College Park), J. Grand'Maison (McGill, Canada), N. Murisic (NJIT), J. Nangle (Arizona), J. Phillips (McGill, Canada), F. Posta (NJIT)

Summary Presentation: C. Raymond, 16 June 2006.

Report Preparation: D.A. Edwards

1 Introduction

In order to implement automated control of a robot arm, it is critical to have an accurate description of the arm's position, orientation, and velocity in 3-space. Such a description can be facilitated with data about how the arm is aligned with the gravitational and magnetic fields of the Earth, which will determine two of the axes in the *Earth frame* E.

Using three accelerometers, TIAX can provide data on the orientation of the Earth's gravitational field with respect to the *body frame* B of the robot arm. The accelerometers are aligned in a *sensor frame* S which may not be orthogonal. However, the processes by which the accelerometer data are calibrated, converted into gravitational measurements, and transformed into an orthogonal basis are proprietary. Therefore, for the purposes of this report, we consider the input to be the body frame data.

Similarly, three magnetometers are used to provide data on the orientation of the Earth's magnetic field with respect to the body frame and three gyroscopes are used to provide data on the angular velocities of each axis making up the body frame.

In this work, we focus on the transformation of this data from the body frame B into the Earth frame E. As described above, the process by which the input (body frame data) is determined is proprietary, and the process which uses the output (Earth frame data) to determine the robot's position can vary with the consumer. However, we do provide some suggestions for handling these processes in Section 9.

We examine the transformations in four different contexts, as described more fully in the following sections:

1. Euler angles
2. Quaternions
3. Rotations about a single axis

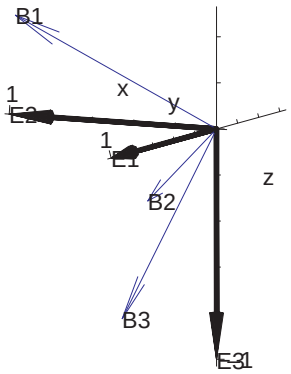

Figure 1: Body and earth frames for $(\phi, \theta, \psi) = (\pi/6, \pi/6, \pi/3)$.

4. Transition matrices

We find that the contexts that do not rely upon angle definitions are superior. Unfortunately, the consumers often demand the contexts that do.

2 The Euler Angle Formulation

In order to control a robot, engineers must know the position and velocity of its various components in the rest frame of the earth E. However, since the sensors are mounted on the device, we can obtain measurements only in the *body frame* B.

We assume both coordinate systems to be associated with unit vectors $\mathbf{B}_i$ and $\mathbf{E}_i$ respectively, where $i = 1, 2, 3$. Each coordinate system is further assumed to be right-handed. Since the sensor body is considered to be cylindrical, we assume that $\mathbf{B}_1$ is aligned along the axis of the cylinder. $\mathbf{E}_1$ is chosen to be aligned to the horizontal component of magnetic north, and $\mathbf{E}_3$ is chosen to point downward. (See Figure 1).

Measurements $\mathbf{G}^{\mathrm{B}}$ (where the superscript "B" stands for "body frame") are taken from accelerometers and measurements $\mathbf{H}^{\mathrm{B}}$ are taken from magnetometers. In order to transform these measurements into the earth frame, we introduce the standard change-of-coordinates matrix ${}_{\mathrm{E}\leftarrow\mathrm{B}}T$, defined by

$$\mathbf{G}^{\mathrm{E}} = {}_{\mathrm{E}\leftarrow\mathrm{B}}T\ \mathbf{G}^{\mathrm{B}}, \tag{1}$$

where the superscript "E" stands for "Earth frame." The same relation holds for $\mathbf{H}$. Note that since we are implementing a rotation, ${}_{\mathrm{E}\leftarrow\mathrm{B}}T$ is an orthogonal matrix, so

$${}_{\mathrm{E}\leftarrow\mathrm{B}}T = {}_{\mathrm{E}\leftarrow\mathrm{B}}T^{-1} = {}_{\mathrm{E}\leftarrow\mathrm{B}}T^{T} \tag{2}$$

Currently, in order to understand the position of the robot arm, the customer requires a set of *Euler angles*, which decompose the rotation into three separate rotations about three separate axes. (These Euler angles are then fed into other software to determine position and velocity.)

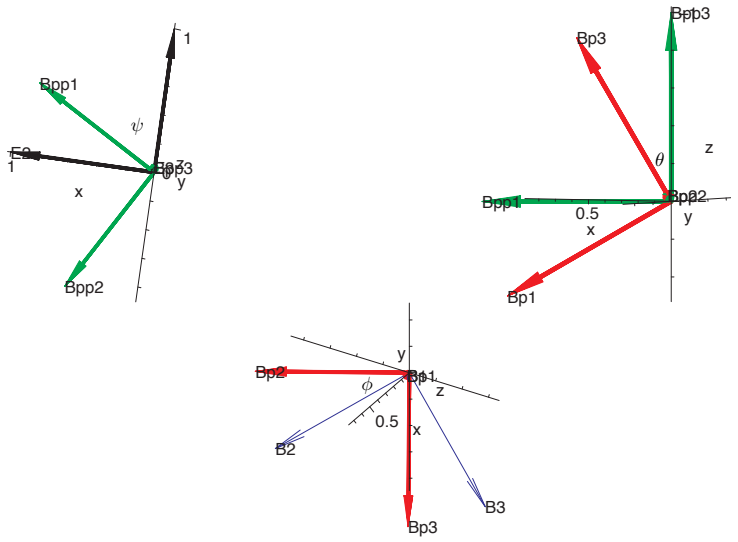

Figure 2: Euler-angle decomposition for $(\phi, \theta, \psi) = (\pi/6, \pi/6, \pi/3)$. In each case, we look down along the axis of rotation. Note that each angle is measured in the proper direction when viewed from the tip of the axis vector.

For the purposes of this manuscript, we assume that the Euler angles are the ones that transform the Earth frame into the body frame. This seems to be different from what TIAX does currently, but is consistent with most of the literature. For our purposes, we will use the sequence of steps which is (believe it or not) alternately called the "xyz convention" in [1] or the "zyx convention" (by most of the rest of the civilized world).

In particular, first the Earth frame is rotated a *heading* (or *yaw*) angle $\psi \in [-\pi, \pi)$ about the $\mathbf{E}_3$-axis (negative z-axis) to form the intermediate frame B$''$ (the notation is historical). (See Figure 2.)

Next, the intermediate frame B$''$ is rotated a *pitch angle* $\theta \in [-\pi/2, \pi/2]$ about the $\mathbf{B}''_2$ axis to form a new intermediate frame B$'$. Note that

1. The length of the interval is only π; the reason for this reduction will be explained below.

2. In some of the literature, θ is restricted to lie in $[0, \pi]$. However, this seems to be the proper choice for other conventions—for the convention we are using, this is the proper choice.

3. The choice of interval ensures that $\cos\theta \geq 0$.

Finally, the intermediate frame B$'$ is rotated a *roll angle* $\phi \in [-\pi, \pi)$ about the $\mathbf{B}'_1$ axis to obtain the body frame B.

Because we are rotating about the "z-axis" of our E-coordinate system first, then the

resulting "y-axis", then the resulting "x-axis", this motivates the terminology "zyx convention".

Mathematically, the Euler-angle method decomposes the transition matrix as follows:

$$ {}_{\mathrm{B}\leftarrow\mathrm{E}}\underline{T} = {}_{\mathrm{B}\leftarrow\mathrm{B}'}\underline{T}\ {}_{\mathrm{B}'\leftarrow\mathrm{B}''}\underline{T}\ {}_{\mathrm{B}''\leftarrow\mathrm{E}}\underline{T} \ . \tag{3} $$

For simplicity of notation, we define the following matrices:

$$ E_\phi = {}_{\mathrm{B}\leftarrow\mathrm{B}'}\underline{T} = \begin{pmatrix} 1 & 0 & 0 \\ 0 & \cos\phi & \sin\phi \\ 0 & -\sin\phi & \cos\phi \end{pmatrix} \tag{4} $$

$$ E_\theta = {}_{\mathrm{B}'\leftarrow\mathrm{B}''}\underline{T} = \begin{pmatrix} \cos\theta & 0 & -\sin\theta \\ 0 & 1 & 0 \\ \sin\theta & 0 & \cos\theta \end{pmatrix} \tag{5} $$

$$ E_\psi = {}_{\mathrm{B}''\leftarrow\mathrm{E}}\underline{T} = \begin{pmatrix} \cos\psi & \sin\psi & 0 \\ -\sin\psi & \cos\psi & 0 \\ 0 & 0 & 1 \end{pmatrix} \tag{6} $$

Note that:

1. Each matrix contains only one of the Euler angles.
2. Each matrix is orthogonal (for instance, $E_\theta^{-1} = E_\theta^T$).
3. The inverse of each matrix is equivalent to rotating through the negative angle (for instance, $E_\phi^{-1} = E_{-\phi} = E_\phi^T$). This convention makes sense only if $\theta \in [-\pi/2, \pi/2]$.

At first glance, it may seem that the signs in E_θ are not consistent with the other two matrices. However, if we treat the rows cyclically, then the last row of E_θ plays the same role as the second row in E_ϕ, and hence it contains the positive $\sin\theta$ term.

To verify that this is indeed the proper direction, we refer to Figure 3, which shows the first rotation from the E frame to the B$''$ frame to the E frame. Examine the triangle with hypotenuse along $\mathbf{E}_1$. Note that the coordinates of the end of the $\mathbf{E}_1$ arrow will have coordinates $(1, 0, 0)$ in the E frame, but $(\cos\psi, -\sin\psi, 0)$ in the B$''$ frame. Thus the transition matrix interpretation is now correct. Moreover, if one examines the triangle with hypotenuse along $\mathbf{B}_1''$, we see that $\mathbf{B}_1'' = \mathbf{E}_1\cos\psi + \mathbf{E}_2\sin\psi$, which is another check.

With these definitions, we have

$$ {}_{\mathrm{B}\leftarrow\mathrm{E}}\underline{T} = E_\phi\, E_\theta\, E_\psi \ . \tag{7} $$

Thus, due to the nature of the matrix multiplication, the matrix corresponding to the "x-rotation" comes first, then the "y-rotation", then the z-rotation. This motivates the naming of this decomposition as the "xyz convention" in [1].

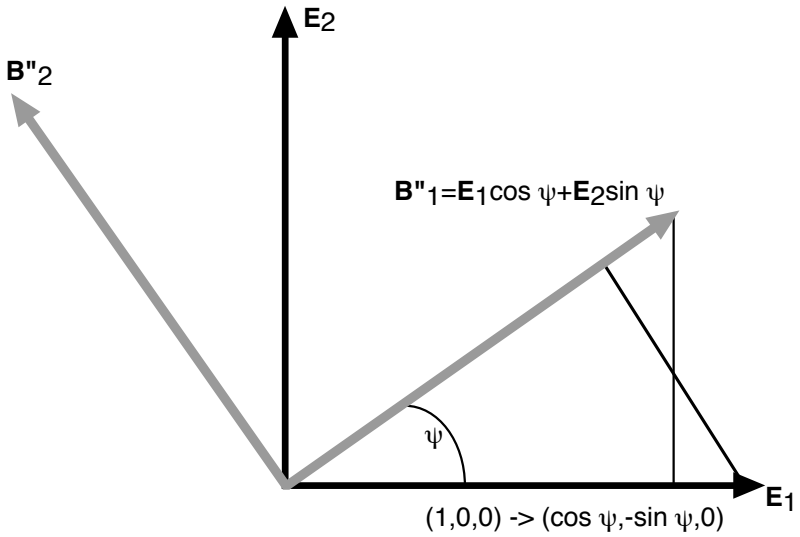

Figure 3: Rotation about z-axis.

Performing the multiplication in (7), we obtain

$$ {}_{\mathrm{B}\leftarrow\mathrm{E}}\underline{T} = \begin{pmatrix} \cos\theta\cos\psi & \cos\theta\sin\psi & -\sin\theta \\ \sin\phi\sin\theta\cos\psi - \cos\phi\sin\psi & \sin\phi\sin\theta\sin\psi + \cos\phi\cos\psi & \sin\phi\cos\theta \\ \cos\phi\sin\theta\cos\psi + \sin\phi\sin\psi & \cos\phi\sin\theta\sin\psi - \sin\phi\cos\psi & \cos\phi\cos\theta \end{pmatrix} . \quad (8) $$

This result may be compared favorably to the result in [1], equation (A.11xyz) if we note that

1. Our notation switches the roles of ψ and ϕ. That is, in [1] ϕ is yaw and ψ is roll.
2. The third edition of [1] has a typo in the lower-left entry; the entry is correct in the second edition.

However, for our purposes it is more useful to have the inverse transformation ${}_{\mathrm{E}\leftarrow\mathrm{B}}\underline{T}$, which is given by

$$ {}_{\mathrm{E}\leftarrow\mathrm{B}}\underline{T} = {}_{\mathrm{B}\leftarrow\mathrm{E}}\underline{T}^{T} = \begin{pmatrix} \cos\theta\cos\psi & \sin\phi\sin\theta\cos\psi - \cos\phi\sin\psi & \cos\phi\sin\theta\cos\psi + \sin\phi\sin\psi \\ \cos\theta\sin\psi & \sin\phi\sin\theta\sin\psi + \cos\phi\cos\psi & \cos\phi\sin\theta\sin\psi - \sin\phi\cos\psi \\ -\sin\theta & \sin\phi\cos\theta & \cos\phi\cos\theta \end{pmatrix} . \quad (9) $$

We now verify mathematically that ϕ and θ are chosen to align the downward axis. We note that with $\mathbf{E}_3$ pointing down,

$$ \mathbf{G}^{\mathrm{E}} = \begin{pmatrix} 0 \\ 0 \\ g \end{pmatrix} , \quad (10) $$

where g is the acceleration of gravity. This is actually true only in the ideal case. With measurement errors included, the constant g in (10) would be replaced by $|\mathbf{G}^{\mathrm{E}}|$, which would vary. However, for the purposes of this manuscript we assume that $|\mathbf{G}^{\mathrm{E}}| = g$. This assumption affects only our error analysis, and will be discussed further in the next section.

Substituting this result into (1) and using our result in (2), we obtain

$$\mathbf{G}^{\mathrm{B}} = {}_{\mathrm{E}\leftarrow\mathrm{B}}\underline{T}^{T} \begin{pmatrix} 0 \\ 0 \\ g \end{pmatrix} , \tag{11}$$

$$\begin{pmatrix} G_1^{\mathrm{B}} \\ G_2^{\mathrm{B}} \\ G_3^{\mathrm{B}} \end{pmatrix} = g \begin{pmatrix} t_{31} \\ t_{32} \\ t_{33} \end{pmatrix} , \tag{12}$$

where t_{ij} is the ijth entry of ${}_{\mathrm{E}\leftarrow\mathrm{B}}\underline{T}$. (Note the transposition operator above.) Then substituting our result in (8) into the above, we have

$$\begin{pmatrix} G_1^{\mathrm{B}} \\ G_2^{\mathrm{B}} \\ G_3^{\mathrm{B}} \end{pmatrix} = g \begin{pmatrix} -\sin\theta \\ \sin\phi\cos\theta \\ \cos\phi\cos\theta \end{pmatrix} . \tag{13}$$

From the first equation, we have

$$\theta = -\sin^{-1}\left(\frac{G_1^{\mathrm{B}}}{g}\right) . \tag{14}$$

Note that

1. Since we are performing a rotation, $|\mathbf{G}^{B}| = g$, so the equation is well-defined.
2. Equation (14) defines θ uniquely in the region $[-\pi/2, \pi/2]$, as asserted above.
3. As long as $|\theta| \neq \pi/2$, the second and third equations in (13) determine ϕ uniquely in $[-\pi, \pi)$. (Both equations are necessary to determine the proper quadrant.)
4. If $|\theta| = \pi/2$, the second and third equations in (13) have right-hand side zero and ϕ cannot be determined uniquely.

This last item is one downside to the Euler-angle decomposition. Algebraically, this can also be seen by substituting $\theta = \pi/2$ into (9), in which case we obtain

$$\begin{aligned} {}_{\mathrm{E}\leftarrow\mathrm{B}}\underline{T}(\theta = \pi/2) &= \begin{pmatrix} 0 & \sin\phi\cos\psi - \cos\phi\sin\psi & \cos\phi\cos\psi + \sin\phi\sin\psi \\ 0 & \sin\phi\sin\psi + \cos\phi\cos\psi & \cos\phi\sin\psi - \sin\phi\cos\psi \\ 1 & 0 & 0 \end{pmatrix} \\ &= \begin{pmatrix} 0 & \sin(\phi-\psi) & \cos(\phi-\psi) \\ 0 & \cos(\phi-\psi) & -\sin(\phi-\psi) \\ 1 & 0 & 0 \end{pmatrix} . \end{aligned} \tag{15}$$

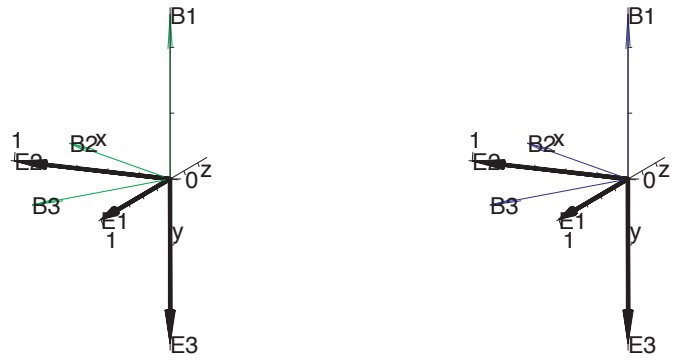

(a) (b)

Figure 4: Degeneracy of Euler-angle decomposition for $\theta = \pi/2$: (a) $(\phi, \psi) = (2\pi/3, \pi/2)$, (b) $(\phi, \psi) = (\pi/3, \pi/6)$.

Therefore, in this case ϕ and ψ cannot be determined explicitly; only their difference can be determined uniquely. (See Figure 4; the results for $\theta = -\pi/2$ are similar.) Note from Figure 4 that in the case presented, $\mathbf{B}_1 = -\mathbf{E}_3$. This alignment of the $\mathbf{B}_1$ and $\mathbf{E}_3$ axes is typical. In this special case, only two rotations are needed to move to the Earth frame; the third is superfluous.

Thus, in any neighborhood of $\theta = \pm\pi/2$, ϕ and ψ take on all of their values. In this sense, these two points are essential singularities in terms of Euler angles. The situation is much the same as what happens on the earth where all values of longitude are attained in any neighborhood of the north and south poles ($\pm\pi/2$ latitude).

Nonetheless, one may be able to recover the values of both ϕ and ψ at $\theta = \pm\pi/2$ in a limiting sense as the robot arm moves toward the singular values in θ. The existence of this trajectory limit depends on whether the arm either moves transversely to $\theta = \pm\pi/2$, in which case ϕ and ψ change slowly and approach limiting values, or conversely the arm spirals into the singularities at $\theta = \pm\pi/2$, in which case ϕ and ψ change rapidly as $\theta \to \pm\pi/2$. This result is particularly important if the robot arm physically can move *to* but not *through* $\theta = \pm\pi/2$.

However, this is simply an artifact of the way we chose to decompose our rotation; the rotation itself is unique. As will be seen later, the method of quaternion vectors avoids this problem. To show that the degeneracy leads to a discontinuity, consider the following problem:

$$\mathbf{G}^{\mathrm{B}} = g \begin{pmatrix} \sqrt{1-\epsilon^2} \\ 0 \\ \epsilon \end{pmatrix} , \ |\epsilon| \ll 1. \tag{16}$$

From (13) we see that as $|\epsilon| \to 0$, $\sin\theta \to -1^+$, so $\theta \to (-\pi/2)^+$. Moreover, $\sin\phi = 0$, so $\phi = 0$ or $\phi = \pi$. Since $\cos\theta > 0$, we have from the last equation that $\cos\phi$ has the same

sign as ϵ, so we have

$$\lim_{\epsilon \to 0^+} \phi = 0, \qquad \lim_{\epsilon \to 0^-} \phi = \pi. \tag{17}$$

In the error section we will address the sensitivity of the angle calculations to the coordinates of $\mathbf{G}^B$.

Lastly, we demonstrate mathematically that ψ is chosen to align the magnetic axis. Assuming that θ and ϕ have already been calculated, we may use (7) to break our transition problem for $\mathbf{H}$ in (1) into known and unknown parts, as follows:

$$\mathbf{H}^{\mathrm{E}} = \begin{pmatrix} H_1^{\mathrm{E}} \\ 0 \\ H_3^{\mathrm{E}} \end{pmatrix} = {}_{\mathrm{E}}\underline{T}_{\mathrm{B}} \mathbf{H}^{\mathrm{B}} = E_\psi^T E_\theta^T E_\phi^T \mathbf{H}^{\mathrm{B}}, \tag{18}$$

$$E_\psi \begin{pmatrix} H_1^{\mathrm{E}} \\ 0 \\ H_3^{\mathrm{E}} \end{pmatrix} = E_\theta^T E_\phi^T \begin{pmatrix} H_1^{\mathrm{B}} \\ H_2^{\mathrm{B}} \\ H_3^{\mathrm{B}} \end{pmatrix}, \tag{19}$$

where we have used the fact that $\mathbf{E}_1$ is aligned with the horizontal component of magnetic north to conclude that $H_2^{\mathrm{E}} = 0$. (This also implies that $H_1^{\mathrm{E}} \neq 0$.) Since the right-hand side is known, in principle ψ may be calculated from (19). The details are left for the next section.

3 Implementation and Error Analysis for Euler Angles

Next we describe how to actually compute the Euler angles given the sensor data, as well as the errors incurred. θ has already been calculated in (14). Now taking the ratio of the last two components of (13), we obtain

$$\frac{G_2^{\mathrm{B}}}{G_3^{\mathrm{B}}} = \tan\phi \tag{20}$$

$$\phi = \tan^{-1}\left(\frac{G_2^{\mathrm{B}}}{G_3^{\mathrm{B}}}\right), \quad \mathrm{sgn}(\phi) = \mathrm{sgn}(G_2^{\mathrm{B}}), \tag{21}$$

where the second equality comes from the fact that $\cos\theta \geq 0$.

Calculating ψ is a little bit trickier. For future reference, we compute the matrix on the right-hand side:

$$\begin{aligned} E_\theta^T E_\phi^T &= \begin{pmatrix} \cos\theta & 0 & \sin\theta \\ 0 & 1 & 0 \\ -\sin\theta & 0 & \cos\theta \end{pmatrix} \begin{pmatrix} 1 & 0 & 0 \\ 0 & \cos\phi & -\sin\phi \\ 0 & \sin\phi & \cos\phi \end{pmatrix} \\ &= \begin{pmatrix} \cos\theta & \sin\theta\sin\phi & \sin\theta\cos\phi \\ 0 & \cos\phi & -\sin\phi \\ -\sin\theta & \cos\theta\sin\phi & \cos\theta\cos\phi \end{pmatrix}. \end{aligned} \tag{22}$$

Substituting our results from (4)-(6) and (22) into (19) and extracting only the first two equations, we have that

$$\begin{pmatrix} \cos\psi & \sin\psi & 0 \\ -\sin\psi & \cos\psi & 0 \\ 0 & 0 & 1 \end{pmatrix} \begin{pmatrix} H_1^{\mathrm{E}} \\ 0 \\ H_3^{\mathrm{E}} \end{pmatrix} = \begin{pmatrix} \cos\theta & \sin\theta\sin\phi & \sin\theta\cos\phi \\ 0 & \cos\phi & -\sin\phi \\ -\sin\theta & \cos\theta\sin\phi & \cos\theta\cos\phi \end{pmatrix} \begin{pmatrix} H_1^{\mathrm{B}} \\ H_2^{\mathrm{B}} \\ H_3^{\mathrm{B}} \end{pmatrix}$$

$$H_1^{\mathrm{E}} \begin{pmatrix} \cos\psi \\ -\sin\psi \end{pmatrix} = \begin{pmatrix} H_1^{\mathrm{B}}\cos\theta + H_2^{\mathrm{B}}\sin\theta\sin\phi + H_3^{\mathrm{B}}\sin\theta\cos\phi \\ H_2^{\mathrm{B}}\cos\phi - H_3^{\mathrm{B}}\sin\phi \end{pmatrix} \quad (23)$$

Taking the ratio of these components, we have

$$-\tan\psi = \frac{H_2^{\mathrm{B}}\cos\phi - H_3^{\mathrm{B}}\sin\phi}{H_1^{\mathrm{B}}\cos\theta + H_2^{\mathrm{B}}\sin\theta\sin\phi + H_3^{\mathrm{B}}\sin\theta\cos\phi}$$

$$\psi = -\tan^{-1}\left(\frac{y_1}{y_2}\right) , \quad (24)$$

where

$$y_1 = H_2^{\mathrm{B}}\cos\phi - H_3^{\mathrm{B}}\sin\phi , \quad (25)$$

$$y_2 = H_1^{\mathrm{B}}\cos\theta + H_2^{\mathrm{B}}\sin\theta\sin\phi + H_3^{\mathrm{B}}\sin\theta\cos\phi . \quad (26)$$

Unfortunately, (24) determines ψ only up to a factor of π. In other words, $\psi \pm \pi$ (whichever is in the proper range) also satisfies (24). When computing ϕ, we used facts about the sign of certain coefficients to aid us. We can do this here only by knowing the sign of H_1^{E}. On a physical level, with one value of ψ, the magnetometer readings have a positive projection along magnetic north. Since ψ rotates the horizontal axes, with ψ having the opposite value, the magnetometer readings have a negative projection along magnetic north.

In order to resolve the discrepancy, we require that $H_1^{\mathrm{E}} \geq 0$, so the magnetometer's poles are aligned with magnetic north. Then using that fact in (24), we have

$$\mathrm{sgn}(\psi) = -\mathrm{sgn}(y_1) \quad (27)$$

from the second component of (23).

Now that the angles have been computed, we would like to see how errors in the measurements $\mathbf{G}^{\mathrm{B}}$ and $\mathbf{H}^{\mathrm{B}}$ affect the measurements of the angles. (We were told that the measurements in any of the components could be expected to have an error of around 1%.) We proceed in order of increasing difficulty, beginning with θ.

Our expression for $d\theta$ can be determined easily from (14) as long as we assume that $|\mathbf{G}^B|$ is always equal to g. If we allow it to vary, then we would have to take differentials of the magnitude of our vector as well. The process for doing that is outlined in section 6. However, for the rest of the manuscript, we assume that $|\mathbf{G}^B|$ is always equal to g. Physically, we are assuming that the accelerometer data we receive as input has already been rescaled such that it has magnitude g, and it is the error in this scaled data that we use in our analysis.

Proceeding with this assumption, we note that since θ is a function only of G_1^{B}, we have

$$\begin{aligned} g\sin\theta &= -G_1^{\mathrm{B}} \\ g\cos\theta\, d\theta &= -dG_1^{\mathrm{B}} \\ d\theta &= -\frac{dG_1^{\mathrm{B}}}{g\cos\theta} \qquad (28) \\ d\theta &= -\frac{dG_1^{\mathrm{B}}}{g\sqrt{1-(G_1^{\mathrm{B}}/g)^2}} = -\frac{dG_1^{\mathrm{B}}}{\sqrt{g^2-(G_1^{\mathrm{B}})^2}}\,, \qquad (29) \end{aligned}$$

where we can choose the positive square root since $\cos\theta \geq 0$. Equation (28) is the easiest to compute (since θ has already been calculated), while (29) has the advantage that it is strictly in terms of the data given. Note that the highest sensitivity occurs when $|\theta| \to \pi/2$ (or equivalently, $|G_1^{\mathrm{B}}| = g$, which means that the sensor is pointing straight up or straight down).

Now let $G_1^{\mathrm{B}} = g - dG_1^{\mathrm{B}}$. (Note the differential has to be negative, since $|\mathbf{G}^{\mathrm{B}}| = g$.) Substituting this expression into (29) and expanding, we have

$$d\theta = -\frac{(-dG_1^{\mathrm{B}})}{\sqrt{g^2-(g-dG_1^{\mathrm{B}})^2}} = \frac{dG_1^{\mathrm{B}}}{\sqrt{2gdG_1^{\mathrm{B}}+\cdots}} = O\left(\sqrt{dG_1^{\mathrm{B}}}\right),$$

so errors in θ remain bounded as $|\theta| \to \pi/2$. This is consistent with our discussion in the previous section, since the discontinuities were in the other angles.

ϕ is a function of G_2^{B} and G_3^{B} only, so we have

$$\begin{aligned} d(\tan\phi) &= \frac{\partial}{\partial G_2^{\mathrm{B}}}\left(\frac{G_2^{\mathrm{B}}}{G_3^{\mathrm{B}}}\right) dG_2^{\mathrm{B}} + \frac{\partial}{\partial G_3^{\mathrm{B}}}\left(\frac{G_2^{\mathrm{B}}}{G_3^{\mathrm{B}}}\right) dG_3^{\mathrm{B}} \\ \sec^2\phi\, d\phi &= \frac{dG_2^{\mathrm{B}}}{G_3^{\mathrm{B}}} - \frac{G_2^{\mathrm{B}}\, dG_3^{\mathrm{B}}}{(G_3^{\mathrm{B}})^2} \\ d\phi &= \cos^2\phi \frac{G_3^{\mathrm{B}}\, dG_2^{\mathrm{B}} - G_2^{\mathrm{B}}\, dG_3^{\mathrm{B}}}{(G_3^{\mathrm{B}})^2} \qquad (30) \\ d\phi &= \frac{G_3^{\mathrm{B}}\, dG_2^{\mathrm{B}} - G_2^{\mathrm{B}}\, dG_3^{\mathrm{B}}}{(G_3^{\mathrm{B}})^2[1+(G_2^{\mathrm{B}}/G_3^{\mathrm{B}})^2]} = \frac{G_3^{\mathrm{B}}\, dG_2^{\mathrm{B}} - G_2^{\mathrm{B}}\, dG_3^{\mathrm{B}}}{(G_2^{\mathrm{B}})^2+(G_3^{\mathrm{B}})^2}. \qquad (31) \end{aligned}$$

In the limit that $|\theta| \to \pi/2$, G_2^{B} and G_3^{B} tend to zero. But the limit in (31) is dependent on how these quantities tend to zero.

To see this, consider

$$\lim_{(G_2^{\mathrm{B}},G_3^{\mathrm{B}})\to(0,0)} \frac{G_3^{\mathrm{B}}\, dG_2^{\mathrm{B}} - G_2^{\mathrm{B}}\, dG_3^{\mathrm{B}}}{(G_2^{\mathrm{B}})^2+(G_3^{\mathrm{B}})^2}.$$

To study the dependence of this limit on the path, suppose first that $G_3^{\mathrm{B}} = mG_2^{\mathrm{B}}$ for some fixed value m. Then G_2^{B} cancels top and bottom, and

$$\lim_{(G_2^{\mathrm{B}},G_3^{\mathrm{B}})\to(0,0)} \frac{G_3^{\mathrm{B}}\, dG_2^{\mathrm{B}} - G_2^{\mathrm{B}}\, dG_3^{\mathrm{B}}}{(G_2^{\mathrm{B}})^2+(G_3^{\mathrm{B}})^2} = \lim_{G_2^{\mathrm{B}}\to 0} \frac{m\, dG_2^{\mathrm{B}} - dG_3^{\mathrm{B}}}{(1+m^2)G_2^{\mathrm{B}}}.$$

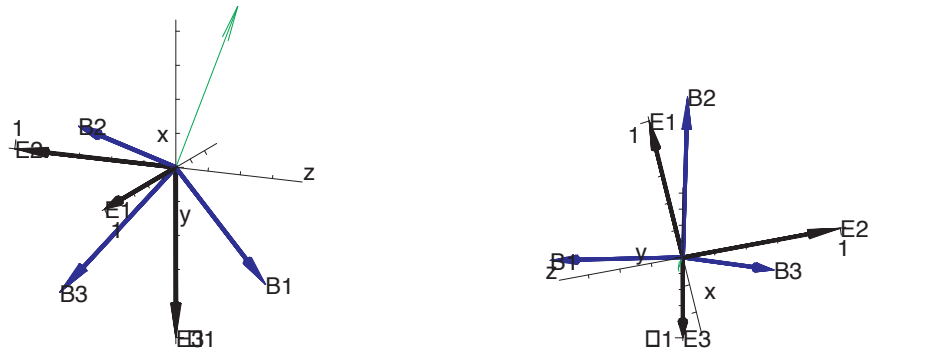

(a) (b)

Figure 5: Rotation interpreted in $(\mathbf{v}, \Phi)$ context for $(\phi, \theta, \psi) = (\pi/6, \pi/6, \pi/3)$: (a) $\mathbf{v}$ (regular arrow) overlaid on Figure 1. (b) Looking down $\mathbf{v}$.

Clearly this result is ill-defined for any m. Hence the error in (31) is not well-defined in that limit, which is consistent with ϕ not having a well-defined value in that limit, either.

The calculation of the errors for ψ are hardest of all, since ψ is a function of $\mathbf{H}$ and $\mathbf{G}$ (through ϕ and θ). If we use arguments analogous to those in (30) and (31), we obtain

$$d\psi = -\cos^2\psi \frac{y_2\, dy_1 - y_1\, dy_2}{y_2^2} \tag{32}$$

$$d\psi = -\frac{y_2\, dy_1 - y_1\, dy_2}{y_1^2 + y_2^2} \ , \tag{33}$$

where

$$dy_1 = \cos\phi\, dH_2^{\mathrm{B}} - \sin\phi\, dH_3^{\mathrm{B}} - (H_2^{\mathrm{B}} \sin\phi + H_3^{\mathrm{B}} \cos\phi)\, d\phi \ , \tag{34}$$

$$dy_2 = \cos\theta\, dH_1^{\mathrm{B}} + \sin\theta \sin\phi\, dH_2^{\mathrm{B}} + \sin\theta \cos\phi\, dH_3^{\mathrm{B}} + (H_2^{\mathrm{B}} \sin\phi + H_3^{\mathrm{B}} \cos\phi) \cos\theta\, d\theta + (-H_1^{\mathrm{B}} \sin\theta + H_2^{\mathrm{B}} \cos\theta \sin\phi + H_3^{\mathrm{B}} \cos\theta \cos\phi)\, d\theta \ , \tag{35}$$

and $d\theta$ and $d\phi$ are given in (28),(29) and (32), (33). Because of the contribution from $d\phi$, the same types of large errors will occur here as $|\theta| \to \pi/2$.

4 Using Quaternion Vectors

The change of reference frame from B to E is simply a matter of rotating the coordinate frame an angle $\Phi \in [0, 2\pi)$ about some axis (represented by unit vector $\mathbf{v}$). (The choice of range will be discussed later. This is the notation in [1]; see Figure 5.) This is the mathematical underpinning of the *quaternion vector* approach. There are several ways to formulate it.

We note that under the mapping $(\theta, \phi, \psi) \mapsto (\psi, \theta, \phi)$, the matrix in [2], equation (13) is exactly ${}_{\mathrm{E}}\underline{T}_{\mathrm{B}}$. Therefore, we may quote this result:

$$ {}_{\mathrm{E}}\underline{T}_{\mathrm{B}} = \begin{pmatrix} v_1^2(1-\cos\Phi)+\cos\Phi & v_1v_2(1-\cos\Phi)-v_3\sin\Phi & v_1v_3(1-\cos\Phi)+v_2\sin\Phi \\ v_1v_2(1-\cos\Phi)+v_3\sin\Phi & v_2^2(1-\cos\Phi)+\cos\Phi & v_2v_3(1-\cos\Phi)-v_1\sin\Phi \\ v_1v_3(1-\cos\Phi)-v_2\sin\Phi & v_2v_3(1-\cos\Phi)+v_1\sin\Phi & v_3^2(1-\cos\Phi)+\cos\Phi \end{pmatrix} , \tag{36} $$

where

$$ v_1^2 + v_2^2 + v_3^2 = 1 \ . \tag{37} $$

to ensure that the transition matrix is orthogonal.

Since

$$ \cos(2\pi - \Phi) = \cos\Phi, \qquad \sin(2\pi - \Phi) = -\sin\Phi, $$

the matrix above is invariant under the mapping $(\mathbf{v}, \Phi) \mapsto (-\mathbf{v}, 2\pi - \Phi)$. This makes physical sense, since in that case the rotations are the same.

The expression for $\mathbf{v}$ can be embedded in a quaternion vector $\mathbf{q} = (q_0, q_1, q_2, q_3)$ as follows:

$$ \mathbf{q} \ = \ \left(\cos\frac{\Phi}{2}, v_1\sin\frac{\Phi}{2}, v_2\sin\frac{\Phi}{2}, v_3\sin\frac{\Phi}{2} \right) \ , \tag{38} $$

$$ \text{with} \qquad q_0^2 + q_1^2 + q_2^2 + q_3^2 = 1 \ , \tag{39} $$

which follows immediately from (37). Note that given a quaternion vector, we would use the arccos function to determine Φ. Thus the range of the arccos is what motivates the choice of $\Phi \in [0, \pi]$.

Since

$$ \cos\frac{2\pi - \Phi}{2} = -\cos\frac{\Phi}{2}, \qquad \sin\frac{2\pi - \Phi}{2} = \sin\frac{\Phi}{2}, $$

we see that $\mathbf{q} \mapsto -\mathbf{q}$ under the mapping $(\mathbf{v}, \Phi) \mapsto (-\mathbf{v}, 2\pi - \Phi)$, which we know corresponds to the same rotation. This *double-covering* of all possible rotations is what allows the quaternions to be free of the type of discontinuities discussed in the previous section. In particular, it is always possible to make the quaternions locally continuous (at the expense of the $\mathbf{q}$ to $-\mathbf{q}$ non-uniqueness globally). That isn't possible for the Euler angles, which cannot be made locally continuous at $\phi = \pi/2$.

However, note that the ordered pair $(\mathbf{v}, \Phi)$ will *not* be continuous in the data. In particular, if we restrict Φ to $[0, \pi]$, there will be some rotation where Φ jumps from 0 to π (or equivalently, $\mathbf{v}$ jumps to $-\mathbf{v}$).

Alternatively, we may follow the analysis in [1], p. 155, in which case we have

$$ {}_{\mathrm{E}}\underline{T}_{\mathrm{B}} = \begin{pmatrix} q_0^2+q_1^2-q_2^2-q_3^2 & 2(q_1q_2-q_0q_3) & 2(q_1q_3+q_0q_2) \\ 2(q_1q_2+q_0q_3) & q_0^2-q_1^2+q_2^2-q_3^2 & 2(q_2q_3-q_0q_1) \\ 2(q_1q_3-q_0q_2) & 2(q_2q_3+q_0q_1) & q_0^2-q_1^2-q_2^2+q_3^2 \end{pmatrix} , \tag{40} $$

since we want the transpose of the matrix in (4.47′) in [1]. Keeping in mind the mapping $(\phi, \psi) \mapsto (\psi, \phi)$ to match with that text, the expressions in (A.13xyz) on p. 604 become

$$q_0 = \cos\frac{\phi}{2}\cos\frac{\theta}{2}\cos\frac{\psi}{2} + \sin\frac{\phi}{2}\sin\frac{\theta}{2}\sin\frac{\psi}{2}, \tag{41}$$

$$q_1 = \sin\frac{\phi}{2}\cos\frac{\theta}{2}\cos\frac{\psi}{2} - \cos\frac{\phi}{2}\sin\frac{\theta}{2}\sin\frac{\psi}{2}, \tag{42}$$

$$q_2 = \cos\frac{\phi}{2}\sin\frac{\theta}{2}\cos\frac{\psi}{2} + \sin\frac{\phi}{2}\cos\frac{\theta}{2}\sin\frac{\psi}{2}, \tag{43}$$

$$q_3 = -\sin\frac{\phi}{2}\sin\frac{\theta}{2}\cos\frac{\psi}{2} + \cos\frac{\phi}{2}\cos\frac{\theta}{2}\sin\frac{\psi}{2}. \tag{44}$$

To check our calculations, we checked the value of ${}_{\mathrm{E}\leftarrow\mathrm{B}}T$ given by (8) and (40) for $(\phi, \theta, \psi) = (\pi/3, \pi/4, \pi/6)$.

Note that using the quaternion group does not remove the singularity if we decide to move back into the Euler angles. In particular, we let $\theta = \pi/2 - \epsilon$ $(0 < \epsilon \ll 1)$ and note that

$$\sin\left(\frac{\pi}{4} - \frac{\epsilon}{2}\right) \sim \frac{1}{\sqrt{2}}\left(1 - \frac{\epsilon}{2}\right), \qquad \cos\left(\frac{\pi}{4} - \frac{\epsilon}{2}\right) \sim \frac{1}{\sqrt{2}}\left(1 + \frac{\epsilon}{2}\right). \tag{45}$$

Then substituting (45) in (41)-(44), we have

$$\begin{aligned} q_0 &= \frac{1}{\sqrt{2}}\left[\cos\frac{\phi}{2}\left(1 + \frac{\epsilon}{2}\right)\cos\frac{\psi}{2} + \sin\frac{\phi}{2}\left(1 - \frac{\epsilon}{2}\right)\sin\frac{\psi}{2}\right] \\ &= \frac{1}{\sqrt{2}}\cos\frac{\phi - \psi}{2} + \frac{1}{2\sqrt{2}}\cos\left(\frac{\phi + \psi}{2}\right)\epsilon + O(\epsilon^2)\ , \end{aligned} \tag{46}$$

$$\begin{aligned} q_1 &= \frac{1}{\sqrt{2}}\left[\sin\frac{\phi}{2}\left(1 + \frac{\epsilon}{2}\right)\cos\frac{\psi}{2} - \cos\frac{\phi}{2}\left(1 - \frac{\epsilon}{2}\right)\sin\frac{\psi}{2}\right] \\ &= \frac{1}{\sqrt{2}}\sin\frac{\phi - \psi}{2} + \frac{1}{2\sqrt{2}}\sin\left(\frac{\phi + \psi}{2}\right)\epsilon + O(\epsilon^2)\ , \end{aligned} \tag{47}$$

$$\begin{aligned} q_2 &= \frac{1}{\sqrt{2}}\left[\cos\frac{\phi}{2}\left(1 - \frac{\epsilon}{2}\right)\cos\frac{\psi}{2} + \sin\frac{\phi}{2}\left(1 + \frac{\epsilon}{2}\right)\sin\frac{\psi}{2}\right] \\ &= \frac{1}{\sqrt{2}}\cos\frac{\phi - \psi}{2} - \frac{1}{2\sqrt{2}}\cos\left(\frac{\phi + \psi}{2}\right)\epsilon + O(\epsilon^2)\ , \end{aligned} \tag{48}$$

$$\begin{aligned} q_3 &= \frac{1}{\sqrt{2}}\left[-\sin\frac{\phi}{2}\left(1 - \frac{\epsilon}{2}\right)\cos\frac{\psi}{2} + \cos\frac{\phi}{2}\left(1 + \frac{\epsilon}{2}\right)\sin\frac{\psi}{2}\right] \\ &= -\frac{1}{\sqrt{2}}\sin\frac{\phi - \psi}{2} + \frac{1}{2\sqrt{2}}\sin\left(\frac{\phi + \psi}{2}\right)\epsilon + O(\epsilon^2)\ . \end{aligned} \tag{49}$$

Therefore, in the limit that $\epsilon \to 0$, we may solve (46)-(49) only for the sum $\psi - \phi$, just as in the previous section. Hence taking a side trip and using the quaternion vectors, only to go back to Euler angles for the customer, doesn't gain us anything from the practical side.

Moreover, if we combine (46)-(49), we obtain

$$\begin{aligned} q_0 - q_2 &= \frac{1}{\sqrt{2}} \cos\left(\frac{\phi+\psi}{2}\right)\epsilon \\ q_1 + q_3 &= \frac{1}{\sqrt{2}} \sin\left(\frac{\phi+\psi}{2}\right)\epsilon \ , \end{aligned}$$

from which we conclude that the left-hand side of each of the above goes to 0 as $\epsilon \to 0$. Continuing to simplify, we have

$$\begin{aligned} (q_0 - q_2)^2 + (q_1 + q_3)^2 &= \frac{\epsilon^2}{2} \\ \sin\left(\frac{\phi+\psi}{2}\right) &= \frac{q_1+q_3}{\sqrt{(q_0-q_2)^2+(q_1+q_3)^2}} \\ \frac{\phi+\psi}{2} &= \sin^{-1}\left(\frac{q_1+q_3}{\sqrt{(q_0-q_2)^2+(q_1+q_3)^2}}\right) \ , \end{aligned} \tag{50}$$

which is in the 0/0 indeterminate form as $\epsilon \to 0$. In particular, it has the form

$$\lim_{(x,y)\to(0,0)} \frac{x}{\sqrt{x^2+y^2}},$$

which is a well-known limit from multivariable calculus. In particular, it approaches a value between -1 and 1 as $(x, y) \to (0, 0)$ transversely, but approaches no fixed value as (x, y) spirals into $(0, 0)$.

This problem can also be seen if we establish the inverse relationships to (41)-(44). This is most easily done by identifying components of (40) with components of (9). In particular, working with the last element of the first column, we have

$$\begin{aligned} 2(q_1q_3 - q_0q_2) &= -\sin\theta \\ \theta &= \sin^{-1}(2(q_0q_2 - q_1q_3)) \ . \end{aligned} \tag{51}$$

Working with the rest of the first column, we have

$$\begin{aligned} q_0^2 + q_1^2 - q_2^2 - q_3^2 &= \cos\theta\cos\psi \\ 2(q_1q_2 + q_0q_3) &= \cos\theta\sin\psi \\ \psi &= \tan^{-1}\left(\frac{2(q_1q_2+q_0q_3)}{q_0^2+q_1^2-q_2^2-q_3^2}\right), \quad \mathrm{sgn}(\psi) = \mathrm{sgn}(q_1q_2+q_0q_3) \ , \end{aligned} \tag{52}$$

where the second equality comes from the fact that $\cos\theta \geq 0$. Working with the rest of the last row, we have

$$\begin{aligned} 2(q_2q_3 + q_0q_1) &= \sin\phi\cos\theta \\ q_0^2 - q_1^2 - q_2^2 + q_3^2 &= \cos\phi\cos\theta \\ \phi &= \tan^{-1}\left(\frac{2(q_2q_3+q_0q_1)}{q_0^2-q_1^2-q_2^2+q_3^2}\right), \quad \mathrm{sgn}(\phi) = \mathrm{sgn}(q_2q_3+q_0q_1) \ , \end{aligned} \tag{53}$$

where the second equality comes from the fact that $\cos\theta \geq 0$.

5 Implementation and Error Analysis for the Quaternions

v and Φ are perhaps more useful for physical interpretation rather than for conversion to the Euler angles. Thus, in practice we may work with the Goldstein formulation (40). To begin, we define the ijth entry of ${}_{\mathrm{E}\leftarrow\mathrm{B}}T$ by t_{ij}. Then we note from (40) that

$$\begin{aligned} t_{13}+t_{31} &= 4q_1q_3 \ , && (54)\\ t_{13}-t_{31} &= 4q_0q_2 \ , && (55)\\ t_{11}+t_{33} &= 2(q_0^2-q_2^2) \ , && (56)\\ t_{11}-t_{33} &= 2(q_1^2-q_3^2) \ . && (57) \end{aligned}$$

Using the definitions above, some algebraic manipulation yields the following four quadratic equations:

$$\begin{aligned} 16(q_0^2)^2-8(t_{11}+t_{33})q_0^2-(t_{13}-t_{31})^2 &= 0 \ , && (58)\\ 16(q_1^2)^2-8(t_{11}-t_{33})q_1^2-(t_{13}+t_{31})^2 &= 0 \ , && (59)\\ 16(q_2^2)^2+8(t_{11}+t_{33})q_2^2-(t_{13}-t_{31})^2 &= 0 \ , && (60)\\ 16(q_3^2)^2+8(t_{11}-t_{33})q_3^2-(t_{13}+t_{31})^2 &= 0 \ . && (61) \end{aligned}$$

Using the quadratic formula and keeping in mind that $q_i^2 \geq 0$ we obtain the solutions:

$$\begin{aligned} q_0^2 &= \frac{1}{4}\left(t_{11}+t_{33}+\sqrt{(t_{11}+t_{33})^2+(t_{13}-t_{31})^2}\right) \ , && (62)\\ q_1^2 &= \frac{1}{4}\left(t_{11}-t_{33}+\sqrt{(t_{11}-t_{33})^2+(t_{13}+t_{31})^2}\right) \ , && (63)\\ q_2^2 &= -\frac{1}{4}\left(t_{11}+t_{33}-\sqrt{(t_{11}+t_{33})^2+(t_{13}-t_{31})^2}\right) \ , && (64)\\ q_3^2 &= -\frac{1}{4}\left(t_{11}-t_{33}-\sqrt{(t_{11}-t_{33})^2+(t_{13}+t_{31})^2}\right) \ . && (65) \end{aligned}$$

However, these equations are useless for the implementation unless we have a relationship between the t_{ij} and the **G** and **H** measurements. For t_{31} and t_{33}, those relationships are given directly by (12):

$$\begin{aligned} t_{31} &= \frac{G_1^{\mathrm{B}}}{g} \ , && (66)\\ t_{33} &= \frac{G_3^{\mathrm{B}}}{g} \ . && (67) \end{aligned}$$

For the **H** calculation, we manipulate (18) and examine simply the first and second com-

ponents:

$$\begin{pmatrix} H_1^{\rm B} \\ H_2^{\rm B} \\ H_3^{\rm B} \end{pmatrix} = {}_{\rm E\leftarrow B}T^T \begin{pmatrix} H_1^{\rm E} \\ 0 \\ H_3^{\rm E} \end{pmatrix} = \begin{pmatrix} t_{11}H_1^{\rm E} + t_{31}H_3^{\rm E} \\ \cdots \\ t_{13}H_1^{\rm E} + t_{33}H_3^{\rm E} \end{pmatrix}$$

$$t_{11}H_1^{\rm E} = H_1^{\rm B} - \frac{G_1^{\rm B}H_3^{\rm E}}{g}$$

$$t_{13}H_1^{\rm E} = H_3^{\rm B} - \frac{G_3^{\rm B}H_3^{\rm E}}{g}$$

$$t_{11} = \frac{gH_1^{\rm B} - G_1^{\rm B}H_3^{\rm E}}{gH_1^{\rm E}}\ , \tag{68}$$

$$t_{13} = \frac{gH_3^{\rm B} - G_3^{\rm B}H_3^{\rm E}}{gH_1^{\rm E}}\ . \tag{69}$$

Note that the second coordinates of $\mathbf{G}$ and $\mathbf{H}$ do not factor directly into the equation; rather, they are handled by the scaling conditions that $|\mathbf{G}|$ and $|\mathbf{H}|$ are constant no matter the reference frame. These equations can also be derived directly from the transition matrix; see section 6.

With (66)-(67) and (68)-(69) in hand, one can easily solve any of (58)-(61) for one of the q_i^2. In finishing the solution process for the remaining quantities q_i, care must be taken to ensure that the algebraic signs of the components of the quaternion are consistently chosen. In particular, we note from our previous discussion that both $\mathbf{q}$ and $-\mathbf{q}$ correspond to the same rotation.

Once q_0 has been determined, then (55) (which is then a linear equation) can be used to determine the unique value of q_2. Unfortunately, we cannot just solve (63) for q_1 and proceed, because then we couldn't be sure that our signs are consistent. Therefore, we now do introduce G_2 directly by examining the second component of (12):

$$t_{32} = \frac{G_2^{\rm B}}{g}\ . \tag{70}$$

Then combining (66),(67) and (70) using (40), we have

$$\begin{aligned} q_2t_{31} - q_1t_{32} &= q_2[2q_2(q_1q_3 - q_0q_2)] - 2q_1[q_2q_3 + q_0q_1] \\ \frac{q_2G_1^{\rm B} - q_1G_2^{\rm B}}{g} &= -2q_0(q_2^2 + q_1^2) = q_0(q_0^2 - q_1^2 - q_2^2 + q_3^2 - 1) = q_0(t_{33} - 1) \\ q_2G_1^{\rm B} - q_1G_2^{\rm B} &= q_0(G_3^{\rm B} - g). \end{aligned} \tag{71}$$

q_1 can then be determined from (71). Finally once q_0, q_1, and q_2 are determined, the unique value of q_3 can be determined from (54).

To estimate errors in the values of the components of the quaternion as functions of the input data $(\mathbf{G}^{\rm B}, \mathbf{H}^{\rm B})$, we must first compute the partial derivatives of the t_{ij} with respect to the data. Using (66), (67) and (68)-(69), we obtain

$$\frac{\partial t_{3i}}{\partial G_j^{\rm B}} = \frac{\delta_{ij}}{g}, \qquad \frac{\partial t_{3i}}{\partial H_j^{\rm B}} = 0, \qquad \frac{\partial t_{1i}}{\partial G_j^{\rm B}} = -\frac{\delta_{ij}H_3^{\rm E}}{gH_1^{\rm E}}, \qquad \frac{\partial t_{1i}}{\partial H_j^{\rm B}} = \frac{\delta_{ij}}{H_1^{\rm E}}, \quad i,j = 1,3, \tag{72}$$

where δ_{ij} is the Kronecker delta function. Note that none of our expressions depend on the measurements in the $\mathbf{B}_2$ direction; this is because these measurements are constrained by the fact that $|\mathbf{G}|$ and $|\mathbf{H}|$ must be constant.

To complete the error analysis of q_0, we now compute the differential (58) with respect to the data. (The computations of the other q_j are similar, especially due to the similar underlying structure of all of (58)-(61)). Taking the differential, we have

$$64q_0^3\,dq_0 - 8\left[(dt_{11}+dt_{33})q_0^2 + 2(t_{11}+t_{33})q_0\,dq_0\right] - 2(t_{13}-t_{31})(dt_{13}-dt_{31}) = 0$$

$$\begin{aligned} 8q_0[4q_0^2-(t_{11}+t_{33})]\,dq_0 &= 4(dt_{11}+dt_{33})q_0^2 + (t_{13}-t_{31})(dt_{13}-dt_{31}) \\ dq_0 &= \frac{4(dt_{11}+dt_{33})q_0^2 + (t_{13}-t_{31})(dt_{13}-dt_{31})}{16q_0[2q_0^2-(t_{11}+t_{33})]}, \end{aligned} \tag{73}$$

where

$$dt_{ij} = \frac{\partial t_{ij}}{\partial G_1^{\mathrm{B}}}\,dG_1^{\mathrm{B}} + \frac{\partial t_{ij}}{\partial G_3^{\mathrm{B}}}\,dG_3^{\mathrm{B}} + \frac{\partial t_{ij}}{\partial H_1^{\mathrm{B}}}\,dH_1^{\mathrm{B}} + \frac{\partial t_{ij}}{\partial H_1^{\mathrm{B}}}\,dH_3^{\mathrm{B}} \tag{74}$$

can be determined from (72).

6 Computing the Transition Matrix Directly

We can also use the data immediately to get the transition matrix ${}_{\mathrm{B}\leftarrow\mathrm{E}}\underline{T}_{\mathrm{E}}$. Recall that from the definition of the transition matrix, the columns of ${}_{\mathrm{B}\leftarrow\mathrm{E}}\underline{T}_{\mathrm{E}}$ are given by the B-coordinates of the **E** vectors. But we have from (11) that

$${}_{\mathrm{E}\leftarrow\mathrm{B}}\underline{T}_{\mathrm{B}}\frac{\mathbf{G}^{\mathrm{B}}}{g} = {}_{\mathrm{E}\leftarrow\mathrm{B}}\underline{T}_{\mathrm{B}}\hat{\mathbf{G}}^{\mathrm{B}} = \begin{pmatrix} 0 \\ 0 \\ 1 \end{pmatrix}, \tag{75}$$

where the hat notation is used to indicate a unit vector. So the third column of ${}_{\mathrm{B}\leftarrow\mathrm{E}}\underline{T}_{\mathrm{E}}$ must be $\hat{\mathbf{G}}^{\mathrm{B}}$. (This can also be verified componentwise using (13) and (8).)

Similarly, proceeding in a purely algebraic way, we have from (18)

$$\begin{aligned} {}_{\mathrm{E}\leftarrow\mathrm{B}}\underline{T}_{\mathrm{B}}\,\frac{\mathbf{H}^{\mathrm{B}}}{H_1^{\mathrm{E}}} &= \begin{pmatrix} 1 \\ 0 \\ H_3^{\mathrm{E}}/H_1^{\mathrm{E}} \end{pmatrix} \\ {}_{\mathrm{E}\leftarrow\mathrm{B}}\underline{T}_{\mathrm{B}}\left(\frac{\mathbf{H}^{\mathrm{B}}}{H_1^{\mathrm{E}}} - \frac{H_3^{\mathrm{E}}\,\hat{\mathbf{G}}^{\mathrm{B}}}{H_1^{\mathrm{E}}}\right) = {}_{\mathrm{E}\leftarrow\mathrm{B}}\underline{T}_{\mathrm{B}}\hat{\mathbf{H}}_{\mathrm{p}}^{\mathrm{B}} &= \begin{pmatrix} 1 \\ 0 \\ 0 \end{pmatrix}, \end{aligned} \tag{76}$$

so the vector in parentheses must be the first column. However, the H_j^{E} are *a priori* unknown. Therefore, we move to a geometric context. We see from (76) that we need to remove any component of $\mathbf{H}^{\mathrm{B}}$ in the $\mathbf{G}^{\mathrm{B}}$ direction:

$$\mathbf{H}_{\mathrm{p}}^{\mathrm{B}} = \mathbf{H}^{\mathrm{B}} - (\mathbf{H}^{\mathrm{B}}\cdot\hat{\mathbf{G}}^{\mathrm{B}})\hat{\mathbf{G}}^{\mathrm{B}}, \tag{77}$$

where the subscript "p" stands for "projection". Note that

1. We don't need to normalize the $\hat{\mathbf{G}}^{\mathrm{B}}$ term because $\hat{\mathbf{G}}^{\mathrm{B}}$ is already a unit vector.

2. From (77) and (76), we see that

$$H_3^{\mathrm{E}} = \mathbf{H}^{\mathrm{B}} \cdot \hat{\mathbf{G}}^{\mathrm{B}}, \tag{78}$$
$$H_1^{\mathrm{E}} = |\mathbf{H}^{\mathrm{B}} - (\mathbf{H}^{\mathrm{B}} \cdot \hat{\mathbf{G}}^{\mathrm{B}})\hat{\mathbf{G}}^{\mathrm{B}}|. \tag{79}$$

Then we must normalize the result. Thus we have

$$\hat{\mathbf{H}}_{\mathrm{p}}^{\mathrm{B}} = \frac{\mathbf{H}_{\mathrm{p}}^{\mathrm{B}}}{|\mathbf{H}_{\mathrm{p}}^{\mathrm{B}}|}. \tag{80}$$

To calculate the second column of the transition matrix ${}_{\mathrm{B}\leftarrow\mathrm{E}}\underline{T}$ we note that since it is orthogonal, the columns must be orthonormal. Therefore, the second column can be calculated as the curl of the first two. In particular, we have that

$${}_{\mathrm{B}\leftarrow\mathrm{E}}\underline{T}\left(\hat{\mathbf{G}}^{\mathrm{B}} \times \hat{\mathbf{H}}_{\mathrm{p}}^{\mathrm{B}}\right) = \begin{pmatrix} 0 \\ 0 \\ 1 \end{pmatrix} \times \begin{pmatrix} 1 \\ 0 \\ 0 \end{pmatrix} = \begin{pmatrix} 0 \\ 1 \\ 0 \end{pmatrix} \tag{81}$$

so we have the second column, and hence a representation for the full matrix:

$${}_{\mathrm{B}\leftarrow\mathrm{E}}\underline{T} = \left(\hat{\mathbf{H}}_{\mathrm{p}}^{\mathrm{B}}, \hat{\mathbf{G}}^{\mathrm{B}} \times \hat{\mathbf{H}}_{\mathrm{p}}^{\mathrm{B}}, \hat{\mathbf{G}}^{\mathrm{B}}\right). \tag{82}$$

This expression can be simplified somewhat (since the $\hat{\mathbf{G}}^{\mathrm{B}} \times \hat{\mathbf{G}}^{\mathrm{B}}$ part of the second column will vanish), but we do not do so here. Note that we have chosen $\hat{\mathbf{G}}^{\mathrm{B}} \times \hat{\mathbf{H}}_{\mathrm{p}}^{\mathrm{B}}$ (rather than $\hat{\mathbf{H}}_{\mathrm{p}}^{\mathrm{B}} \times \hat{\mathbf{G}}^{\mathrm{B}}$) to get a right-handed coordinate frame.

Once ${}_{\mathrm{B}\leftarrow\mathrm{E}}\underline{T}$ has been calculated, it is a simple matter to obtain $\mathbf{v}$ and Φ, at least up to a minus sign error. Since ${}_{\mathrm{B}\leftarrow\mathrm{E}}\underline{T}$ is an orthogonal matrix, it must have a real unit eigenvector with eigenvalue 1. This eigenvector must be $\mathbf{v}$, since $\mathbf{v}$ is invariant under the rotation. The other two eigenvalues must be of the form $e^{\pm i\Phi}$, since they describe the rotation about the axis.

The only ambiguity with this system is making sure that you have the right $(\mathbf{v}, \Phi)$ pair and that you haven't accidentally negated one of them. But this is easily checked by substituting the pair into (36) and make sure that the transition matrix ${}_{\mathrm{E}\leftarrow\mathrm{B}}\underline{T}$ is the *transpose* of the matrix in (82).

Alternatively, we may construct $\mathbf{v}$ directly from the transition matrix. In particular, we may calculate Φ as before or by using the fact that

$$\mathrm{tr}\ {}_{\mathrm{B}\leftarrow\mathrm{E}}\underline{T} = 1 + e^{i\Phi} + e^{-i\Phi} = 1 + 2\cos\Phi, \tag{83}$$

which will give us a definite value of Φ, since at this stage we may restrict ourselves to a quadrant.

To construct $\mathbf{v}$, we first consider a unit vector $\mathbf{z} \neq c\mathbf{v}$ for any constant c, and then construct

$$\mathbf{z}_\perp = ({}_{\mathrm{E}\leftarrow\mathrm{B}}\underline{T} - {}_{\mathrm{B}\leftarrow\mathrm{E}}\underline{T})\mathbf{z}. \tag{84}$$

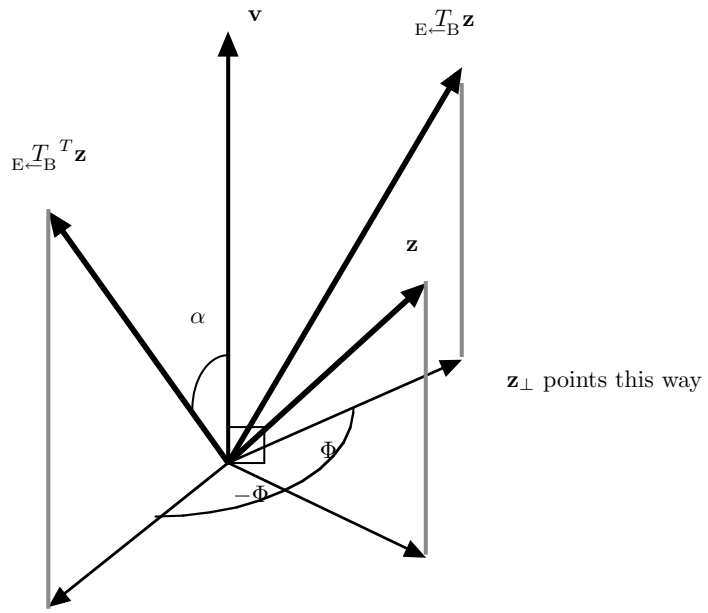

Figure 6: Visualization of **w** under rotation.

We first note that

$$\mathbf{z}_\perp \cdot \mathbf{v} = ({}_{E\leftarrow B}T - {}_{B\leftarrow E}T)\mathbf{z}\cdot\mathbf{v} = \mathbf{z}\cdot({}_{E\leftarrow B}T - {}_{B\leftarrow E}T)^T\mathbf{v} = \mathbf{z}\cdot({}_{B\leftarrow E}T - {}_{E\leftarrow B}T)\mathbf{v} = \mathbf{z}\cdot(\mathbf{v}-\mathbf{v}) = 0,$$

where we have used the fact that **v** is invariant under the rotation. So $\mathbf{z}_\perp \perp \mathbf{v}$. Moreover, we have that

$$\mathbf{z}_\perp \cdot \mathbf{z} = ({}_{E\leftarrow B}T - {}_{B\leftarrow E}T)\mathbf{z}\cdot\mathbf{z} = {}_{E\leftarrow B}T\mathbf{z}\cdot\mathbf{z} - \mathbf{z}\cdot {}_{B\leftarrow E}T^{T}\mathbf{z} = {}_{E\leftarrow B}T\mathbf{z}\cdot\mathbf{z} - {}_{E\leftarrow B}T\mathbf{z}\cdot\mathbf{z} = 0,$$

so $\mathbf{z}_\perp \perp \mathbf{z}$ as well. Thus $\mathbf{z}_\perp$ is a multiple of $\mathbf{v}\times\mathbf{z}$.

To find the multiple, we note that the length of $\mathbf{z}_\perp$ is given by

$$|\mathbf{z}_\perp|^2 = \left|{}_{E\leftarrow B}T\mathbf{z}\right|^2 + \left|{}_{B\leftarrow E}T\mathbf{z}\right|^2 - 2({}_{E\leftarrow B}T\mathbf{z}\cdot{}_{E\leftarrow B}T^{T}\mathbf{z}) = 2\left[1 - {}_{E\leftarrow B}T\mathbf{z}\cdot{}_{E\leftarrow B}T^{T}\mathbf{z}\right]. \tag{85}$$

To calculate the dot product, we next examine Figure 6. We first take the dot product of the projections of ${}_{E\leftarrow B}T^{T}\mathbf{z}$ and ${}_{E\leftarrow B}T\mathbf{z}$ onto the plane perpendicular to **v**:

$$\left[{}_{E\leftarrow B}T^{T}\mathbf{z} - ({}_{E\leftarrow B}T^{T}\mathbf{z}\cdot\mathbf{v})\mathbf{v}\right]\cdot\left[{}_{E\leftarrow B}T\mathbf{z} - ({}_{E\leftarrow B}T\mathbf{z}\cdot\mathbf{v})\mathbf{v}\right]$$

$$= \left|{}_{E\leftarrow B}T^{T}\mathbf{z} - \left({}_{E\leftarrow B}T^{T}\mathbf{z}\cdot\mathbf{v}\right)\right|\left|{}_{E\leftarrow B}T\mathbf{z} - \left({}_{E\leftarrow B}T\mathbf{z}\cdot\mathbf{v}\right)\,\mathbf{v}\right|\cos 2\Phi$$

$$\begin{aligned}{}_{E\leftarrow B}T^{T}\mathbf{z}\cdot{}_{E\leftarrow B}T\mathbf{z} - ({}_{E\leftarrow B}T^{T}\mathbf{z}\cdot\mathbf{v})(\mathbf{v}\cdot{}_{E\leftarrow B}T^{T}\mathbf{z}) \quad &- \quad ({}_{E\leftarrow B}T\mathbf{z}\cdot\mathbf{v})({}_{E\leftarrow B}T^{T}\mathbf{z}\cdot\mathbf{v}) \\ &+ \quad ({}_{E\leftarrow B}T^{T}\mathbf{z}\cdot\mathbf{v})({}_{E\leftarrow B}T\mathbf{z}\cdot\mathbf{v})(\mathbf{v}\cdot\mathbf{v}) = \sin^2\alpha\cos 2\Phi\end{aligned}$$

$$
\begin{aligned}
{}_{\mathrm{E}\leftarrow\mathrm{B}}\underline{T}^{T}_{\mathrm{B}}\mathbf{z}\cdot\,{}_{\mathrm{E}\leftarrow\mathrm{B}}\underline{T}_{\mathrm{B}}\mathbf{z}-({}_{\mathrm{E}\leftarrow\mathrm{B}}\underline{T}_{\mathrm{B}}\mathbf{z}\cdot\mathbf{v})({}_{\mathrm{E}\leftarrow\mathrm{B}}\underline{T}^{T}_{\mathrm{B}}\mathbf{z}\cdot\mathbf{v}) &= \sin^2\alpha(2\cos^2\Phi-1)\\
-\,{}_{\mathrm{E}\leftarrow\mathrm{B}}\underline{T}^{T}_{\mathrm{B}}\mathbf{z}\cdot\,{}_{\mathrm{E}\leftarrow\mathrm{B}}\underline{T}_{\mathrm{B}}\mathbf{z} &= -({}_{\mathrm{E}\leftarrow\mathrm{B}}\underline{T}_{\mathrm{B}}\mathbf{v}\cdot\mathbf{z})({}_{\mathrm{E}\leftarrow\mathrm{B}}\underline{T}^{T}_{\mathrm{B}}\mathbf{v}\cdot\mathbf{z})-\sin^2\alpha(2\cos^2\Phi-1)\\
1-\,{}_{\mathrm{E}\leftarrow\mathrm{B}}\underline{T}_{\mathrm{B}}\mathbf{z}\cdot\,{}_{\mathrm{E}\leftarrow\mathrm{B}}\underline{T}^{T}_{\mathrm{B}}\mathbf{z} &= 1-(\mathbf{v}\cdot\mathbf{z})^2-\sin^2\alpha(2\cos^2\Phi-1)\\
1-\,{}_{\mathrm{E}\leftarrow\mathrm{B}}\underline{T}_{\mathrm{B}}\mathbf{z}\cdot\,{}_{\mathrm{E}\leftarrow\mathrm{B}}\underline{T}^{T}_{\mathrm{B}}\mathbf{z} &= 1-(|\mathbf{v}||\mathbf{z}|\cos\alpha)^2-\sin^2\alpha(2\cos^2\Phi-1)\\
2\left[1-\,{}_{\mathrm{E}\leftarrow\mathrm{B}}\underline{T}_{\mathrm{B}}\mathbf{z}\cdot\,{}_{\mathrm{E}\leftarrow\mathrm{B}}\underline{T}^{T}_{\mathrm{B}}\mathbf{z}\right] &= 2\cdot 2\left[\sin^2\alpha(1-\cos^2\Phi)\right]\ ,
\end{aligned}
$$

where we have used the fact that $\mathbf{v}$ and $\mathbf{z}$ are unit vectors and $\mathbf{v}$ is unaffected by the rotation. Then substituting this result into (85), we obtain

$$|\mathbf{z}_\perp| = 2\sin\alpha\sin\Phi, \tag{86}$$

where we have used the diagram to deduce which sign of $\sin\Phi$ to use.

Then using the definition of the cross product and its matrix representation, we have

$$
\begin{aligned}
\mathbf{z}_\perp &= 2(\mathbf{v}\times\mathbf{z})\sin\Phi\\
\frac{1}{2\sin\Phi}\begin{pmatrix} 0 & t_{12}-t_{21} & t_{13}-t_{31}\\ t_{21}-t_{12} & 0 & t_{23}-t_{32}\\ t_{31}-t_{13} & t_{32}-t_{23} & 0\end{pmatrix}\mathbf{z} &= \begin{pmatrix} 0 & -v_3 & v_2\\ v_3 & 0 & -v_1\\ -v_2 & v_1 & 0\end{pmatrix}\mathbf{z}\\
\mathbf{v} &= \frac{1}{2\sin\Phi}\begin{pmatrix} t_{32}-t_{23}\\ t_{13}-t_{31}\\ t_{21}-t_{12}\end{pmatrix},
\end{aligned}
\tag{87}
$$

which then gives an explicit expression for $\mathbf{v}$ in terms of the t_{ij}.

To perform the error analysis, we first note the trivial facts that

$$\frac{\partial\hat{\mathbf{G}}^{\mathrm{B}}}{\partial G_i^B}=\frac{\mathbf{e}_i}{g},\qquad \frac{\partial\hat{\mathbf{G}}^{\mathrm{B}}}{\partial H_i^B}=\mathbf{0},\qquad \frac{\partial\hat{\mathbf{H}}^{\mathrm{B}}}{\partial G_i^B}=\mathbf{0},\qquad \frac{\partial\hat{\mathbf{H}}^{\mathrm{B}}}{\partial H_i^B}=\frac{\mathbf{e}_i}{|\mathbf{H}^{\mathrm{B}}|}, \tag{88}$$

where $\mathbf{e}_i$ is the ith standard basis vector. Note that for any variable y,

$$
\begin{aligned}
\frac{d}{dy}\left(\frac{1}{|\mathbf{H}^{\mathrm{B}}_{\mathrm{p}}|}\right) &= \frac{d}{dy}\left(\frac{1}{(\mathbf{H}^{\mathrm{B}}_{\mathrm{p}}\cdot\mathbf{H}^{\mathrm{B}}_{\mathrm{p}})^{1/2}}\right)=-\frac{1}{2(\mathbf{H}^{\mathrm{B}}_{\mathrm{p}}\cdot\mathbf{H}^{\mathrm{B}}_{\mathrm{p}})^{3/2}}\frac{d(\mathbf{H}^{\mathrm{B}}_{\mathrm{p}}\cdot\mathbf{H}^{\mathrm{B}}_{\mathrm{p}})}{dy}\\
&= -\frac{1}{2|\mathbf{H}^{\mathrm{B}}_{\mathrm{p}}|^3}\left(2\mathbf{H}^{\mathrm{B}}_{\mathrm{p}}\cdot\frac{d\mathbf{H}^{\mathrm{B}}_{\mathrm{p}}}{dy}\right)=-\frac{1}{|\mathbf{H}^{\mathrm{B}}_{\mathrm{p}}|^2}\left(\hat{\mathbf{H}}^{\mathrm{B}}_{\mathrm{p}}\cdot\frac{d\mathbf{H}^{\mathrm{B}}_{\mathrm{p}}}{dy}\right)\\
\frac{d}{dy}\left(\frac{\mathbf{H}^{\mathrm{B}}_{\mathrm{p}}}{|\mathbf{H}^{\mathrm{B}}_{\mathrm{p}}|}\right) &= \frac{1}{|\mathbf{H}^{\mathrm{B}}_{\mathrm{p}}|}\frac{d\mathbf{H}^{\mathrm{B}}_{\mathrm{p}}}{dy}+\mathbf{H}^{\mathrm{B}}_{\mathrm{p}}\frac{d}{dy}\left(\frac{1}{|\mathbf{H}^{\mathrm{B}}_{\mathrm{p}}|}\right)\\
\frac{d\hat{\mathbf{H}}^{\mathrm{B}}_{\mathrm{p}}}{dy} &= \frac{1}{|\mathbf{H}^{\mathrm{B}}_{\mathrm{p}}|}\frac{d\mathbf{H}^{\mathrm{B}}_{\mathrm{p}}}{dy}-\frac{\hat{\mathbf{H}}^{\mathrm{B}}_{\mathrm{p}}}{|\mathbf{H}^{\mathrm{B}}_{\mathrm{p}}|}\left(\hat{\mathbf{H}}^{\mathrm{B}}_{\mathrm{p}}\cdot\frac{d\mathbf{H}^{\mathrm{B}}_{\mathrm{p}}}{dy}\right)\ .
\end{aligned}
\tag{89}
$$

Now for the variables under consideration, we have

$$\begin{aligned}\frac{\partial \mathbf{H}_{\mathrm{p}}^{\mathrm{B}}}{\partial G_i^{\mathrm{B}}} &= \mathbf{0} - \left[\left(\mathbf{0}\cdot\hat{\mathbf{G}}^{\mathrm{B}} + \mathbf{H}^{\mathrm{B}}\cdot\frac{\mathbf{e}_i}{g}\right)\hat{\mathbf{G}}^{\mathrm{B}} + \left(\mathbf{H}^{\mathrm{B}}\cdot\hat{\mathbf{G}}^{\mathrm{B}}\right)\frac{\mathbf{e}_i}{g}\right] \\ &= -\frac{H_i^{\mathrm{B}}\hat{\mathbf{G}}^{\mathrm{B}} + H_3^{\mathrm{E}}\mathbf{e}_i}{g}\,, \qquad (90)\\ \frac{\partial \mathbf{H}_{\mathrm{p}}^{\mathrm{B}}}{\partial H_i^{\mathrm{B}}} &= \mathbf{e}_i - \left[\left(\mathbf{e}_i\cdot\hat{\mathbf{G}}^{\mathrm{B}} + \mathbf{H}^{\mathrm{B}}\cdot\mathbf{0}\right)\hat{\mathbf{G}}^{\mathrm{B}} + \left(\mathbf{H}^{\mathrm{B}}\cdot\hat{\mathbf{G}}^{\mathrm{B}}\right)\mathbf{0}\right] \\ &= \mathbf{e}_i - \hat{G}_i^{\mathrm{B}}\hat{\mathbf{G}}^{\mathrm{B}}, \qquad (91)\end{aligned}$$

where he have used (78) and (88). Then taking the dot products in (89), we obtain

$$\begin{aligned}\hat{\mathbf{H}}_{\mathrm{p}}^{\mathrm{B}}\cdot\frac{\partial \mathbf{H}_{\mathrm{p}}^{\mathrm{B}}}{\partial G_i^{\mathrm{B}}} &= \hat{\mathbf{H}}_{\mathrm{p}}^{\mathrm{B}}\cdot\left(-\frac{H_i^{\mathrm{B}}\hat{\mathbf{G}}^{\mathrm{B}} + H_3^{\mathrm{E}}\mathbf{e}_i}{g}\right) = -\frac{H_3^{\mathrm{E}}(\hat{H}_{\mathrm{p}}^{\mathrm{B}})_i}{g}, \qquad (92)\\ \hat{\mathbf{H}}_{\mathrm{p}}^{\mathrm{B}}\cdot\frac{\partial \mathbf{H}_{\mathrm{p}}^{\mathrm{B}}}{\partial H_i^{\mathrm{B}}} &= \hat{\mathbf{H}}_{\mathrm{p}}^{\mathrm{B}}\cdot(\mathbf{e}_i - \hat{G}_i^{\mathrm{B}}\hat{\mathbf{G}}^{\mathrm{B}}) = (\hat{H}_{\mathrm{p}}^{\mathrm{B}})_i, \qquad (93)\end{aligned}$$

where we have used the fact that $\mathbf{H}_{\mathrm{p}}^{\mathrm{B}}$ and $\mathbf{G}^{\mathrm{B}}$ are orthogonal.

Substituting (90),(91) and (92),(93) into (89), we obtain

$$\begin{aligned}\frac{\partial \hat{\mathbf{H}}_{\mathrm{p}}^{\mathrm{B}}}{\partial G_i^{\mathrm{B}}} &= \frac{1}{|\mathbf{H}_{\mathrm{p}}^{\mathrm{B}}|}\left[-\frac{H_i^{\mathrm{B}}\hat{\mathbf{G}}^{\mathrm{B}} + H_3^{\mathrm{E}}\mathbf{e}_i}{g}\right] - \frac{\hat{\mathbf{H}}_{\mathrm{p}}^{\mathrm{B}}}{|\mathbf{H}_{\mathrm{p}}^{\mathrm{B}}|}\left(-\frac{H_3^{\mathrm{E}}(\hat{H}_{\mathrm{p}}^{\mathrm{B}})_i}{g}\right) \\ &= -\frac{H_i^{\mathrm{B}}\hat{\mathbf{G}}^{\mathrm{B}} + H_3^{\mathrm{E}}\mathbf{e}_i - H_3^{\mathrm{E}}(\hat{H}_{\mathrm{p}}^{\mathrm{B}})_i\hat{\mathbf{H}}_{\mathrm{p}}^{\mathrm{B}}}{g|\mathbf{H}_{\mathrm{p}}^{\mathrm{B}}|}, \\ &= -\frac{H_3^{\mathrm{E}}\mathbf{z}_i}{g} - \frac{H_i^{\mathrm{B}}\hat{\mathbf{G}}^{\mathrm{B}}}{g|\mathbf{H}_{\mathrm{p}}^{\mathrm{B}}|}, \qquad \mathbf{z}_i = \frac{\mathbf{e}_i - (\hat{H}_{\mathrm{p}}^{\mathrm{B}})_i\hat{\mathbf{H}}_{\mathrm{p}}^{\mathrm{B}}}{|\mathbf{H}_{\mathrm{p}}^{\mathrm{B}}|} \qquad (94)\\ \frac{\partial \hat{\mathbf{H}}_{\mathrm{p}}^{\mathrm{B}}}{\partial H_i^{\mathrm{B}}} &= \frac{\mathbf{e}_i - \hat{G}_i^{\mathrm{B}}\hat{\mathbf{G}}^{\mathrm{B}}}{|\mathbf{H}_{\mathrm{p}}^{\mathrm{B}}|} - \frac{\hat{\mathbf{H}}_{\mathrm{p}}^{\mathrm{B}}(\hat{H}_{\mathrm{p}}^{\mathrm{B}})_i}{|\mathbf{H}_{\mathrm{p}}^{\mathrm{B}}|} = \mathbf{z}_i - \frac{\hat{G}_i^{\mathrm{B}}\hat{\mathbf{G}}^{\mathrm{B}}}{|\mathbf{H}_{\mathrm{p}}^{\mathrm{B}}|}, \qquad (95)\end{aligned}$$

Lastly, to determine the error in the middle column, we compute

$$\begin{aligned}\frac{\partial(\hat{\mathbf{G}}^{\mathrm{B}}\times\hat{\mathbf{H}}_{\mathrm{p}}^{\mathrm{B}})}{\partial G_i^{\mathrm{B}}} &= \frac{\partial\hat{\mathbf{G}}^{\mathrm{B}}}{\partial G_i^{\mathrm{B}}}\times\hat{\mathbf{H}}_{\mathrm{p}}^{\mathrm{B}} + \hat{\mathbf{G}}^{\mathrm{B}}\times\frac{\partial\hat{\mathbf{H}}_{\mathrm{p}}^{\mathrm{B}}}{\partial G_i^{\mathrm{B}}} = \frac{\mathbf{e}_i}{g}\times\hat{\mathbf{H}}_{\mathrm{p}}^{\mathrm{B}} + \hat{\mathbf{G}}^{\mathrm{B}}\times\left[-\frac{H_3^{\mathrm{E}}\mathbf{z}_i}{g} - \frac{H_i^{\mathrm{B}}\hat{\mathbf{G}}^{\mathrm{B}}}{g|\mathbf{H}_{\mathrm{p}}^{\mathrm{B}}|}\right] \\ &= \frac{1}{g}\left[\mathbf{e}_i\times\hat{\mathbf{H}}_{\mathrm{p}}^{\mathrm{B}} - H_3^{\mathrm{E}}(\hat{\mathbf{G}}^{\mathrm{B}}\times\mathbf{z}_i)\right]\,, \\ \frac{\partial(\hat{\mathbf{G}}^{\mathrm{B}}\times\hat{\mathbf{H}}_{\mathrm{p}}^{\mathrm{B}})}{\partial H_i^{\mathrm{B}}} &= \frac{\partial\hat{\mathbf{G}}^{\mathrm{B}}}{\partial H_i^{\mathrm{B}}}\times\hat{\mathbf{H}}_{\mathrm{p}}^{\mathrm{B}} + \hat{\mathbf{G}}^{\mathrm{B}}\times\frac{\partial\hat{\mathbf{H}}_{\mathrm{p}}^{\mathrm{B}}}{\partial H_i^{\mathrm{B}}} = \hat{\mathbf{G}}^{\mathrm{B}}\times\left(\mathbf{z}_i - \frac{\hat{G}_i^{\mathrm{B}}\hat{\mathbf{G}}^{\mathrm{B}}}{|\mathbf{H}_{\mathrm{p}}^{\mathrm{B}}|}\right) = \hat{\mathbf{G}}^{\mathrm{B}}\times\mathbf{z}_i, \qquad (96)\end{aligned}$$

Then with these expressions, we see that the error in the transition matrix ${}_{\mathrm{B}\leftarrow\mathrm{E}}T_{\mathrm{E}}$ is given by

$$d{}_{\mathrm{B}\leftarrow\mathrm{E}}T_{\mathrm{E}} = \sum_{i=1}^{3}\left(\frac{\partial\hat{\mathbf{H}}_{\mathrm{p}}^{\mathrm{B}}}{\partial G_i^{\mathrm{B}}}, \frac{\partial(\hat{\mathbf{G}}^{\mathrm{B}}\times\hat{\mathbf{H}}_{\mathrm{p}}^{\mathrm{B}})}{\partial G_i^{\mathrm{B}}}, \frac{\mathbf{e}_i}{g}\right)dG_i^{\mathrm{B}} + \left(\frac{\partial\hat{\mathbf{H}}_{\mathrm{p}}^{\mathrm{B}}}{\partial H_i^{\mathrm{B}}}, \frac{\partial(\hat{\mathbf{G}}^{\mathrm{B}}\times\hat{\mathbf{H}}_{\mathrm{p}}^{\mathrm{B}})}{\partial H_i^{\mathrm{B}}}, \mathbf{0}\right)dH_i^{\mathrm{B}}. \qquad (97)$$

Note that the transition matrix is smooth in the data, which is correct since the transition matrix is simply made up of numbers with no angles attached.

7 Matlab Implementation

The group has implemented MATLAB programs that test errors due to measurement noise for two of the algorithms in the previous sections.

These programs work with four representations of a rotation:

1. The transition matrix ${}_{\mathrm{B}\leftarrow\mathrm{E}}\underline{T}$.
2. $\mathbf{v}$ and Φ from the quaternion description.
3. The Euler angles.
4. $\mathbf{q}$ from the quaternion description.

We have written subroutines that convert among these representations by direct computation:

1. Given ${}_{\mathrm{B}\leftarrow\mathrm{E}}\underline{T}$, find $\mathbf{v}$ and Φ using the procedure described in section 6.
2. Given ${}_{\mathrm{B}\leftarrow\mathrm{E}}\underline{T}$, find (ϕ, θ, ψ) directly using (9).
3. Given $\mathbf{v}$ and Φ, compute ${}_{\mathrm{B}\leftarrow\mathrm{E}}\underline{T}$ directly using (36).
4. Given $\mathbf{v}$ and Φ, compute $\mathbf{q}$ using (38).
5. Given (ϕ, θ, ψ), compute ${}_{\mathrm{B}\leftarrow\mathrm{E}}\underline{T}$ directly using (9).
6. Given (ϕ, θ, ψ), compute $\mathbf{q}$ directly using (41)-(44).
7. Given $\mathbf{q}$, compute ${}_{\mathrm{B}\leftarrow\mathrm{E}}\underline{T}$ directly using (40).
8. Given $\mathbf{q}$, compute $\mathbf{v}$ and Φ using manipulations of (38).
9. Given $\mathbf{q}$, compute (ϕ, θ, ψ) using (51)-(53).

We have also written subroutines that use the data inputs $\mathbf{G}^{\mathrm{B}}$ and $\mathbf{H}^{\mathrm{B}}$ to compute rotations:

1. Given $\mathbf{G}^{\mathrm{B}}$ and $\mathbf{H}^{\mathrm{B}}$, compute ${}_{\mathrm{B}\leftarrow\mathrm{E}}\underline{T}$ using (82).
2. Given $\mathbf{G}^{\mathrm{B}}$ and $\mathbf{H}^{\mathrm{B}}$, compute $\mathbf{q}$ using Newton's method on the system of nonlinear equations derived by substituting ${}_{\mathrm{B}\leftarrow\mathrm{E}}\underline{T}$ as defined in (40) into (11) and (18).
3. Given $\mathbf{G}^{\mathrm{B}}$ and $\mathbf{H}^{\mathrm{B}}$, compute (ϕ, θ, ψ) using (14), (21), and (24)-(27).

To test errors due to measurement noise, we wrote a simulator that generates the data inputs $\mathbf{G}^{\mathrm{B}}$ and $\mathbf{H}^{\mathrm{B}}$ for a given set of Euler angles, adds random noise, and then uses the subroutines above to try to recover the Euler angles. In the following examples, $\mathbf{G}^{\mathrm{B}}$ and $\mathbf{H}^{\mathrm{B}}$ have measurement noise of 1%. In each case, ψ was fixed at $\pi/4$ and the other Euler angles (θ, ϕ) vary over their full range.

It is possible for spurious errors to arise from these angles approaching the end of their ranges. For example, if ϕ was near 2π and a perturbation in the data would send it to $2\pi + \epsilon$, that angle would be mapped to ϵ, which would (formally) cause a very large error in ϕ.

To eliminate such spurious results, the errors were calculated as follows. Given a set of Euler angles (θ, ϕ), the corresponding $\mathbf{G}^{\mathrm{B}}$ and $\mathbf{H}^{\mathrm{B}}$ values were computed using (13) and (23). Then the transition matrix ${}_{\mathrm{B}\leftarrow\mathrm{E}}T$ was computed using (82). Once the data was perturbed, the perturbed transition matrix ${}_{\mathrm{B}_\Delta\leftarrow\mathrm{E}}T$ was computed, again using (82).

Given these two matrices, the differential angles $(d\phi, d\theta, d\psi)$ are then simply those angles which rotate from the B to B_Δ frames. Hence they be obtained from the transition matrix

$$ {}_{\mathrm{B}_\Delta\leftarrow\mathrm{B}}T = {}_{\mathrm{B}_\Delta\leftarrow\mathrm{E}}T\ {}_{\mathrm{B}\leftarrow\mathrm{E}}T^T. $$

Then we use subroutines 2, above, to convert from the transition matrix to the error angles. Since the transition matrix is smooth in the data and isn't affected by the ranges, the differential angles calculated will hence always be small.

There are several ways that one can compute the perturbed transition matrix. First, one can solve for the angles directly as described in method #3 above. Once the angles have been computed, it is a simple matter to substitute into (9) to obtain the perturbed transition matrix. The errors obtained by such a procedure are shown in Figure 7. Note that each error is comparable in size to the perturbation of the data. Note also that $d\psi$ is somewhat larger than the others, because ψ is dependent on both $\mathbf{G}^{\mathrm{B}}$ and $\mathbf{H}^{\mathrm{B}}$, while the other two angles are dependent only on $\mathbf{G}^{\mathrm{B}}$.

Alternatively, given the perturbed data, one can compute the perturbed transition matrix directly as described in method #1 above. The errors obtained by such a procedure are shown in Figure 8. Given the same random data set, the two methods produce results that are identical down to the floating-point precision. The only reason why Figures 7 and 8 differ is because a different random data set was used for each.

8 Using the Gyroscope

The accelerometer and magnetometer measurements are used to determine the Euler angles at any time t. However, the time rate of change of each of these quantities is also important. Because of various errors associated with computation, it is better to have stand-alone measurements of these, rather than taking differentials of the $\mathbf{G}$ and $\mathbf{H}$ data. Therefore, we compute these quantities from qyroscope data, which yields the quantity

$$ \vec{\omega} = \begin{pmatrix} \omega_1 \\ \omega_2 \\ \omega_3 \end{pmatrix} , \tag{98} $$

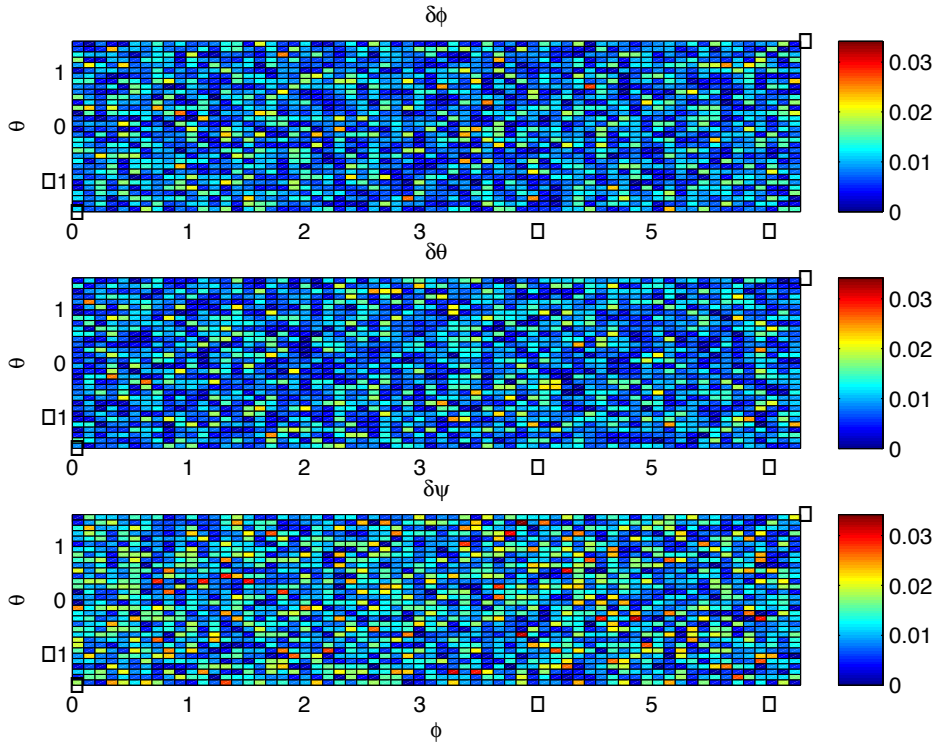

Figure 7: Errors in angle measurements, angles calculated using method #3.

where ω_i is the angular velocity about axis i *in the body frame*. Thus this information needs to be converted into $(\dot{\phi}, \dot{\theta}, \dot{\psi})$, where the dot indicates differentiation with respect to t.

Since ϕ is defined as rotation about $\mathbf{B}_1$, it contributes directly to ω without changing coordinates. Therefore, we write

$$\vec{\omega}_\phi = \begin{pmatrix} \dot{\phi} \\ 0 \\ 0 \end{pmatrix} . \tag{99}$$

Since ω_2 is measured in the B frame and $\dot{\theta}$ is measured in the B′ frame, we must apply the proper transformation matrix to relate the two quantities. Thus we have

$$\vec{\omega}_\theta = {}_{\mathrm{B}}\underleftarrow{T}_{\mathrm{B}'} \begin{pmatrix} 0 \\ \dot{\theta} \\ 0 \end{pmatrix} = E_\phi \begin{pmatrix} 0 \\ \dot{\theta} \\ 0 \end{pmatrix} = \begin{pmatrix} 1 & 0 & 0 \\ 0 & \cos\phi & \sin\phi \\ 0 & -\sin\phi & \cos\phi \end{pmatrix} \begin{pmatrix} 0 \\ \dot{\theta} \\ 0 \end{pmatrix} . \tag{100}$$

Similarly, since ω_3 is measured in the B frame and $\dot{\psi}$ is measured in the B″ frame, we must

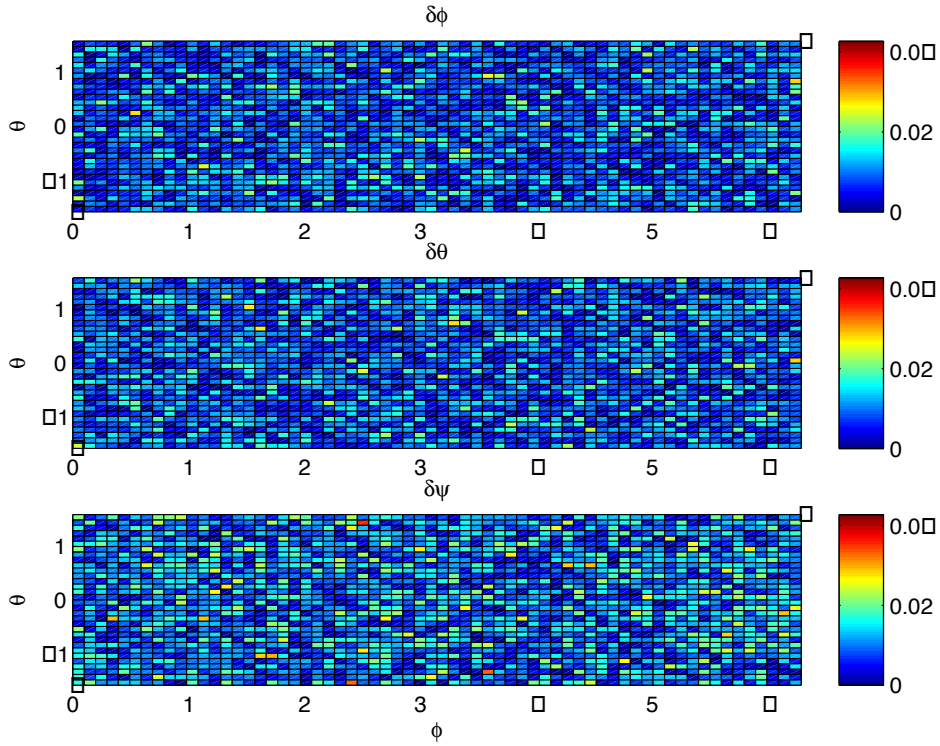

Figure 8: Errors in angle measurements, angles calculated using method #1.

apply the proper transformation matrix to relate the two quantities:

$$\vec{\omega}_\psi = {}_{\mathrm{B}\underline{\leftarrow}\mathrm{B}''}T \begin{pmatrix} 0 \\ 0 \\ \dot{\psi} \end{pmatrix} = E_\phi E_\theta \begin{pmatrix} 0 \\ 0 \\ \dot{\psi} \end{pmatrix} = \begin{pmatrix} \cos\theta & 0 & -\sin\theta \\ \sin\theta\sin\phi & \cos\phi & \cos\theta\sin\phi \\ \sin\theta\cos\phi & -\sin\phi & \cos\theta\cos\phi \end{pmatrix} \begin{pmatrix} 0 \\ 0 \\ \dot{\psi} \end{pmatrix}, \tag{101}$$

where we have used the transpose of (22).

Then adding these quantities to obtain the true gyroscopic data, we have

$$\vec{\omega} = \vec{\omega}_\phi + \vec{\omega}_\theta + \vec{\omega}_\psi = {}_{\mathrm{B}\underline{\leftarrow}\mathrm{E}}W \begin{pmatrix} \dot{\phi} \\ \dot{\theta} \\ \dot{\psi} \end{pmatrix}, \tag{102}$$

$${}_{\mathrm{B}\underline{\leftarrow}\mathrm{E}}W = \begin{pmatrix} 1 & 0 & -\sin\theta \\ 0 & \cos\phi & \cos\theta\sin\phi \\ 0 & -\sin\phi & \cos\theta\cos\phi \end{pmatrix}, \tag{103}$$

where ${}_{\mathrm{B}\underline{\leftarrow}\mathrm{E}}W$ is the transition matrix from E to B *for the angular velocities*. Here we have used the form of the vectors in (99)-(101) to note that the first column of ${}_{\mathrm{B}\underline{\leftarrow}\mathrm{E}}W$ is the first column of the (identity) matrix in (99), the second column is the second column in (100), and the third column is the third column in (101).

Unfortunately, ${}_{\mathrm{B}}\underline{W}_{\mathrm{E}}$ is not orthogonal, so it cannot be inverted just by taking the transpose. Moreover, ${}_{\mathrm{B}}\underline{W}_{\mathrm{E}}$ is not even invertible if $|\theta| = \pi/2$. In this case (which we already know to be problematic), the third column is a multiple of the first.

Nevertheless, for $|\theta| \neq \pi/2$, some work will provide the inverse matrix

$$ {}_{\mathrm{B}}\underline{W}_{\mathrm{E}}^{-1} = {}_{\mathrm{E}}\underline{W}_{\mathrm{B}} = \begin{pmatrix} 1 & \sin\phi\tan\theta & \cos\phi\tan\theta \\ 0 & \cos\phi & -\sin\phi \\ 0 & \sin\phi\sec\theta & \cos\phi\sec\theta \end{pmatrix}, \tag{104} $$

so

$$ \begin{pmatrix} \dot{\phi} \\ \dot{\theta} \\ \dot{\psi} \end{pmatrix} = {}_{\mathrm{E}}\underline{W}_{\mathrm{B}}\vec{\omega}. \tag{105} $$

Note that as promised, the inverse doesn't exist for $|\theta| = \pi/2$.

Since (105) is a linear system, the error analysis is relatively straightforward. First, similar to the argument presented at the beginning of the section, we do not integrate or otherwise use the gyroscope data to compute the Euler angles. Thus we may consider $(\dot{\phi}, \dot{\theta}, \dot{\psi})$ to be independent of (ϕ, θ, ψ) in the following error analysis. Then taking the derivatives, we have

$$ \begin{pmatrix} \dot{\phi} \\ \dot{\theta} \\ \dot{\psi} \end{pmatrix} = \frac{\partial\, {}_{\mathrm{E}}\underline{W}_{\mathrm{B}}}{\partial\phi}\vec{\omega}\, d\phi + \frac{\partial\, {}_{\mathrm{E}}\underline{W}_{\mathrm{B}}}{\partial\theta}\vec{\omega}\, d\theta + {}_{\mathrm{E}}\underline{W}_{\mathrm{B}}\, d\vec{\omega}, \tag{106} $$

$$ \frac{\partial\, {}_{\mathrm{E}}\underline{W}_{\mathrm{B}}}{\partial\phi} = \begin{pmatrix} 0 & \cos\phi\tan\theta & -\sin\phi\tan\theta \\ 0 & -\sin\phi & -\cos\phi \\ 0 & \cos\phi\sec\theta & -\sin\phi\sec\theta \end{pmatrix} \tag{107} $$

$$ \frac{\partial\, {}_{\mathrm{E}}\underline{W}_{\mathrm{B}}}{\partial\theta} = \begin{pmatrix} 0 & \sin\phi\sec^2\theta & \cos\phi\sec^2\theta \\ 0 & 0 & 0 \\ 0 & \sin\phi\tan\theta\sec\theta & \cos\phi\tan\theta\sec\theta \end{pmatrix}, \tag{108} $$

and the errors in the angles are as described in (28) and (30).

We continue by deriving the evolution equations of the quaternions from the gyroscopic data. First, consider the basis vector $\mathbf{B}_1$. In the B coordinate frame, its coordinates are $(1, 0, 0)^T$, the coordinates of $\mathbf{E}_1$ in the standard basis. In other words,

$$ \mathbf{B}_1 = {}_{\mathrm{E}}\underline{T}_{\mathrm{B}}\mathbf{E}_1. $$

Since this is true for each vector, we have (by the properties of the rotation matrix) that

$$ \mathbf{E}_i = {}_{\mathrm{B}}\underline{T}_{\mathrm{E}}\mathbf{B}_i, \quad i = 1, 2, 3. \tag{109} $$

Taking the time derivative of (109) and realizing that the Earth frame never changes, we have

$$ \mathbf{0} = {}_{\mathrm{B}}\underline{\dot{T}}_{\mathrm{E}}\mathbf{B}_i + {}_{\mathrm{B}}\underline{T}_{\mathrm{E}}\dot{\mathbf{B}}_i. \tag{110} $$

But the body frame moves as a result of the angular velocities, so we have

$$\dot{\mathbf{B}}_i = \vec{\omega} \times \mathbf{B}_i. \tag{111}$$

Substituting (111) into (110), we have

$$ {}_{\mathrm{B}}\dot{\underline{T}}_{\mathrm{E}}\mathbf{B}_i + {}_{\mathrm{B}}\underline{T}_{\mathrm{E}}(\vec{\omega} \times \mathbf{B}_i) = \mathbf{0}$$

$$\begin{aligned}
({}_{\mathrm{E}}\dot{\underline{T}}_{\mathrm{B}}^{T} + {}_{\mathrm{E}}\underline{T}_{\mathrm{B}}^{T}\Omega)\mathbf{B}_i &= \mathbf{0}, \qquad \Omega = \begin{pmatrix} 0 & -\omega_3 & \omega_2 \\ \omega_3 & 0 & -\omega_1 \\ -\omega_2 & \omega_1 & 0 \end{pmatrix} \\
{}_{\mathrm{E}}\dot{\underline{T}}_{\mathrm{B}}^{T} &= -{}_{\mathrm{E}}\underline{T}_{\mathrm{B}}^{T}\Omega \\
{}_{\mathrm{E}}\dot{\underline{T}}_{\mathrm{B}} &= \Omega\, {}_{\mathrm{E}}\underline{T}_{\mathrm{B}} \qquad (112) \\
{}_{\mathrm{E}}\underline{T}_{\mathrm{B}}^{T}\, {}_{\mathrm{E}}\dot{\underline{T}}_{\mathrm{B}} &= \Omega, \qquad (113)
\end{aligned}$$

where in deriving (112) we have used the fact that the equation above must be true for all $\mathbf{B}_i$. Here Ω is that matrix which, when multiplied by $\mathbf{B}_i$, always yields the cross product.

Note that since Ω is antisymmetric, (113) is really only three independent equations for the four unknown components of $\dot{\mathbf{q}}$. (The fourth is provided by the derivative of (39).) We note from (54)-(57) that

$$\begin{aligned}
\dot{t}_{13} + \dot{t}_{31} &= 4(\dot{q}_1 q_3 + q_1 \dot{q}_3), \\
\dot{t}_{13} - \dot{t}_{31} &= 4(\dot{q}_0 q_2 + q_0 \dot{q}_2), \\
\dot{t}_{11} + \dot{t}_{33} &= 4(q_0 \dot{q}_0 - q_2 \dot{q}_2), \\
\dot{t}_{11} - \dot{t}_{33} &= 4(q_1 \dot{q}_1 - q_3 \dot{q}_3).
\end{aligned}$$

from which we obtain

$$\begin{aligned}
q_3(\dot{t}_{13} + \dot{t}_{31}) + q_1(\dot{t}_{11} - \dot{t}_{33}) &= 4\dot{q}_1(q_1^2 + q_3^2), \qquad (114) \\
q_0(\dot{t}_{13} - \dot{t}_{31}) - q_2(\dot{t}_{11} + \dot{t}_{33}) &= 4\dot{q}_2(q_0^2 + q_2^2), \qquad (115) \\
q_1(\dot{t}_{13} + \dot{t}_{31}) - q_3(\dot{t}_{11} - \dot{t}_{33}) &= 4\dot{q}_3(q_1^2 + q_3^2), \qquad (116)
\end{aligned}$$

where we have reduced down to three equations for reasons which will become clear later.

For simplicity, we work with (112), which becomes

$$\begin{pmatrix} \dot{t}_{11} & \dot{t}_{12} & \dot{t}_{13} \\ \dot{t}_{21} & \dot{t}_{22} & \dot{t}_{23} \\ \dot{t}_{31} & \dot{t}_{32} & \dot{t}_{33} \end{pmatrix} = \begin{pmatrix} 0 & -\omega_3 & \omega_2 \\ \omega_3 & 0 & -\omega_1 \\ -\omega_2 & \omega_1 & 0 \end{pmatrix} \begin{pmatrix} t_{11} & t_{12} & t_{13} \\ t_{21} & t_{22} & t_{23} \\ t_{31} & t_{32} & t_{33} \end{pmatrix}$$

$$\begin{aligned}
\dot{t}_{11} &= -t_{21}\omega_3 + t_{31}\omega_2, \qquad (117) \\
\dot{t}_{13} &= -t_{23}\omega_3 + t_{33}\omega_2, \qquad (118) \\
\dot{t}_{31} &= -t_{11}\omega_2 + t_{21}\omega_1, \qquad (119) \\
\dot{t}_{33} &= -t_{13}\omega_2 + t_{23}\omega_1. \qquad (120)
\end{aligned}$$

Substituting these results into (114), we have

$$\begin{aligned} 4\dot{q}_1(q_1^2+q_3^2) &= q_3(-t_{11}\omega_2+t_{21}\omega_1-t_{23}\omega_3+t_{33}\omega_2)+q_1(-t_{21}\omega_3+t_{31}\omega_2+t_{13}\omega_2-t_{23}\omega_1) \\ \dot{q}_1 &= \frac{\omega_1(q_3t_{21}-q_1t_{23})+\omega_2[q_3(t_{33}-t_{11})+q_1(t_{31}+t_{13})]-\omega_3(q_3t_{23}+q_1t_{21})}{4(q_1^2+q_3^2)} \\ &= \frac{\omega_1[2q_0(q_1^2+q_3^2)]+\omega_2[2q_3(q_1^2-q_3^2)+q_1(4q_1q_3)]-\omega_3[-2q_2(q_1^2+q_3^2)]}{4(q_1^2+q_3^2)} \\ &= \frac{\omega_1q_0+\omega_2q_3-\omega_3q_2}{2}, \end{aligned} \tag{121}$$

where we have used (40). Using the fact that $(q_1, q_3) \mapsto (-q_3, q_1)$ in the left-hand sides of (114) and (116), we see that (116) becomes

$$\begin{aligned} \dot{q}_3 &= \frac{\omega_1(q_1t_{21}+q_3t_{23})+\omega_2[q_1(t_{33}-t_{11})-q_3(t_{31}+t_{13})]-\omega_3(q_1t_{23}-q_3t_{21})}{4(q_1^2+q_3^2)} \\ &= \frac{\omega_1[2q_2(q_1^2+q_3^2)]+\omega_2[-2q_1(q_1^2-q_3^2)-q_3(4q_1q_3)]-\omega_3[-2q_0(q_1^2+q_3^2)]}{4(q_1^2+q_3^2)} \\ &= \frac{\omega_1q_2-\omega_2q_1+\omega_3q_0}{2}. \end{aligned} \tag{122}$$

Finally, we substitute our results into (115), which yields

$$\begin{aligned} 4\dot{q}_2(q_0^2+q_2^2) &= q_0(-t_{23}\omega_3+t_{33}\omega_2+t_{11}\omega_2-t_{21}\omega_1)-q_2(-t_{21}\omega_3+t_{31}\omega_2-t_{13}\omega_2+t_{23}\omega_1) \\ \dot{q}_2 &= \frac{\omega_1(-q_0t_{21}-q_2t_{23})+\omega_2[q_0(t_{33}+t_{11})-q_2(t_{31}-t_{13})]+\omega_3(-q_0t_{23}+q_2t_{21})}{4(q_0^2+q_2^2)} \\ &= \frac{\omega_1[-2q_3(q_0^2+q_2^2)]+\omega_2[2q_0(q_0^2-q_2^2)-q_2(-4q_0q_2)]+\omega_3[2q_1(q_0^2+q_2^2)]}{4(q_0^2+q_2^2)} \\ &= \frac{-\omega_1q_3+\omega_2q_0+\omega_3q_1}{2}. \end{aligned} \tag{123}$$

With these equations in place, $\dot{q}_0$ can be derived from (39):

$$\begin{aligned} 2q_0\dot{q}_0+2q_1\dot{q}_1+2q_2\dot{q}_2+2q_3\dot{q}_3 &= 0 \\ \dot{q}_0 &= -\frac{(q_1\dot{q}_1+q_2\dot{q}_2+q_3\dot{q}_3)}{q_0}. \end{aligned} \tag{124}$$

The workshop concluded before we had time to derive an error analysis for this case.

9 Conclusions and Further Research

In this work, we have analyzed the relationship between $\mathbf{G}^{\mathrm{B}}$, $\mathbf{H}^{\mathrm{B}}$, and the position of a sensor robot arm. We analyzed the relationship by interpreting the movement in terms of transition matrices, Euler angles, quaternions, and rotations about an axis. We also produced an error analysis of the dependent variables on the data.

Since transition matrices and quaternions are simply made up of scalars, they were found to vary smoothly with the data. On the other hand, once we introduced an angle into the analysis, we immediately ran into several problems.

The first (and perhaps most important) conclusion is that when reviewing the literature on Euler angles, it is critical to understand the "convention" (*i.e.*, the axes and order of rotation) used. This choice will affect the computation of all the parameters in the problem, as well as the ranges of the angles.

In the Euler-angle formulation, an indeterminacy arises when $|\theta| = \pi/2$. In that case (which occurs when $\mathbf{B}_1$ is aligned either straight up or straight down), only two rotations are necessary, so only the difference between ψ and ϕ is measurable. Moreover, in either the Euler-angle or vector-angle descriptions, each angle becomes discontinuous in the data as it nears the end of its range. In contrast, the transition matrices and quaternions (which are based upon trigonometric functions of the angles) vary smoothly with the data.

In short: *The rotation (as represented by* $\mathbf{q}$ *and* T*) is continuous in the data. The man-made convention of choosing angle ranges for* ψ*,* θ*,* ϕ*, and* Φ *makes these variables discontinuous in the data.*

The immediate conclusion from this fact is that quaternions or the rotation matrix is the best way to handle the data. Of the two, using the rotation matrix directly is probably the fastest due to the simplicity with which one can calculate ${}_{\mathrm{B}\leftarrow\mathrm{E}}T$ from the data using (82).

Therefore, one marked improvement could be obtained by implementing an algorithm to interpret the movement of the arm based upon T alone. Though TIAX could implement this as a downstream solution, a major problem is that certain customers, in order to integrate the sensor results into their own systems, require that the Euler angles be output.

We also analyzed the relationship between $\vec{\omega}$ and the movement of a sensor robot arm. We analyzed the relationship by interpreting the movement in terms of derivatives of the Euler angles and quaternions. (Interpretations in terms of transition matrices and rotations about an axis, though beyond the scope of this manuscript, should follow naturally.)

We did complete an error analysis of the gyroscopic data in the Euler-angle formulation and found (not surprisingly) that the variation of $(\dot{\phi}, \dot{\theta}, \dot{\psi})$ with errors in $\vec{\omega}$ was arbitrarily large as $|\theta| \to \pi/2$. We did not have enough time to complete an error analysis of $\dot{\mathbf{q}}$ with the data $\vec{\omega}$. Though our experience leads us to believe that the errors will be smooth, this is a fruitful area for further research.

The measurement errors analyzed in this work vary with each signal, the frequency of which is 60 Hz. In addition, there will also be *calibration errors* associated with these measurements. We list them below, in addition with some strategies for addressing them:

1. Calibration errors in translating the actual data results from the sensor into $\mathbf{G}$, $\mathbf{H}$, and $\vec{\omega}$ in the sensor frame. One source of these errors is temperature variation. However, these variations will occur on a much longer time scale. If the robot is working in an environment with large temperature variations, periodic (twice-daily?) calibrations may be appropriate, if the duration of such calibrations can be made acceptable to consumers.

   Another source of such calibration error may be due to vibrations or large forces (accelerations) in the robot arm. However, this calibration is proprietary to TIAX,

so we have no further information on the process.

2. Calibration errors in transforming the sensor frame to an orthogonal coordinate system. Again, this calibration is proprietary, so it is unclear how much vibrations or other accelerations may affect the orientations of the sensors. If there is little effect, then again an occasional calibration should be appropriate.

3. Calibration errors in aligning the orthogonal sensor frame with the body frame. Since we have no guarantee that (with errors as described in #2) the sensor frame will always be transformed in to the *same* orthogonal frame, this is a separate issue that must be considered. However, since this is just a rotation between two orthogonal frames, the mathematical analysis should be quite similar to the sort described in this report.

4. Calibration errors in aligning the Earth frame (as interpreted by the alignment software) to the actual Earth coordinate system. Note that neither of these frames is moving in relationship to one another. Thus, one should be able to eliminate such errors by doing a simple displacement calculation, rather than working from an absolute zero. Any drift that might occur (perhaps due to vibrations induced during the robot's work cycle) will occur on a very slow time scale. Again, a periodic calibration may be necessary.

5. Errors associated with scaling $|\mathbf{G}|$ to have length g. These can be addressed directly using techniques similar to those described in section 6; the group just ran out of time before analyzing them.

Nomenclature

If the same letter appears both in bold and plain text, the variables in plain text are components of the vector which appears in bold. The equation number where a particular quantity first appears is listed, if appropriate.

B: unit vector describing orientation of body frame.

E: unit vector describing orientation of earth frame.

E**:** intermediate rotation matrix (4).

e: standard basis vector (88).

G: vector of accelerometer measurements.

g**:** acceleration of gravity (10).

H: vector of magnetometer measurements.

i**:** indexing variable.

j**:** indexing variable.

q: quaternion vector (38).

${}_{\mathrm{E}\leftarrow\mathrm{B}}T$**:** transition matrix for coordinates from body frame to earth frame (1).

t**:** element of ${}_{\mathrm{E}\leftarrow\mathrm{B}}T$ (12).

v: unit vector corresponding to axis of rotation.

${}_{\mathrm{B}\leftarrow\mathrm{E}}W$**:** transition matrix for angular velocities from Earth frame to body frame (103).

x**:** dummy variable.

y**:** dummy variable (25),(26).

z: intermediate vector, variously defined (94).

$\mathcal{Z}$**:** the integers.

δ_{ij}**:** Kronecker delta function (72).

ϵ**:** small parameter, variously defined (45).

θ**:** pitch angle of rotation about $\mathbf{B}_2'$.

Φ**:** combined angle of rotation.

ϕ**:** roll angle of rotation about $\mathbf{B}_1$.

ψ**:** heading (yaw) angle of rotation about $\mathbf{B}_3''$.

Ω**:** matrix representing $\vec{\omega}\times$ (112).

$\vec{\omega}$**:** vector of gyroscope measurements (98).

Other Notation

B**:** as a superscript, used to indicate the body frame.

E**:** as a superscript, used to indicate the earth frame.

$n \in \mathcal{Z}$**:** as a subscript, used to indicate a direction in a reference frame or as an index for a dummy variable (25).

p**:** as a subscript on $\mathbf{H}^{\mathrm{B}}$, used to indicate a projection (76).

$\perp$**:** as a subscript, used to denote orthogonality (84).

ϕ**:** as a subscript on E, used to refer to the ϕ rotation (4).

ψ**:** as a subscript on E, used to refer to the ψ rotation (6).

θ**:** as a subscript on E, used to refer to the ψ rotation (5).

$\dot{}$**:** used to indicate differentiation with respect to t.

$\hat{}$**:** used to indicate a unit vector (75).

$'$**:** used to indicate first intermediate frame.

$''$**:** used to indicate second intermediate frame.

References

[1] Goldstein, H., Poole, C., and Safko, J. *Classical Mechanics*, 3rd ed., San Francisco: Addison Wesley, 2002.

[2] Mukundan, R. Quaternions: From Classical Mechanics to Computer Graphics, and Beyond. *Proc. of Asian Technology Conference in Mathematics: ATCM2002*, Malaysia (Dec. 2002), pp. 97–106.